

NO-0105 830

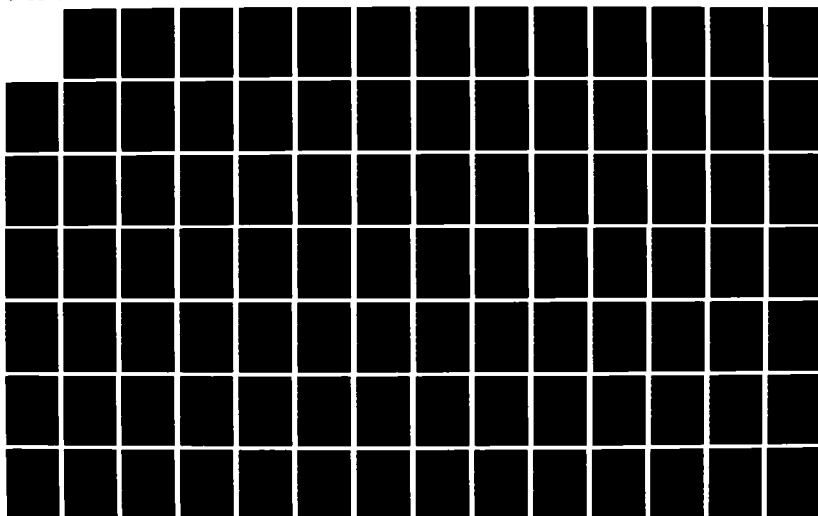
QUADRATURE-QUADRATURE PHASE SHIFT KEYING(U) HIGHWAY
UNIV ANN ARBOR COMMUNICATIONS AND SIGNAL PROCESSING LAB
D SAHM SEP 86 021779-3-T N00014-04-K-0066

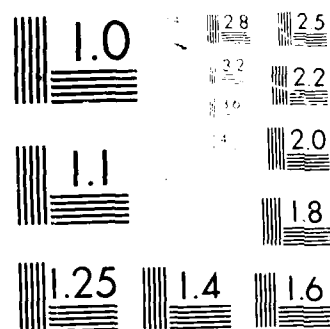
1/2

UNCLASSIFIED

F/B 25/5

ML



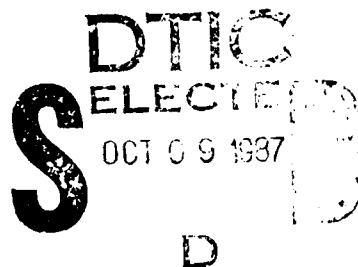


AD-A185 838

Report 021779-3-T

QUADRATURE-QUADRATURE PHASE SHIFT KEYING

D. Saha



COMMUNICATIONS & SIGNAL PROCESSING LABORATORY

Department of Electrical Engineering and Computer Science
The University of Michigan
Ann Arbor, Michigan 48109

September 1986

Technical Report No. 240

Approved for public release; distribution unlimited.

Prepared for

OFFICE OF NAVAL RESEARCH

Department of the Navy
Arlington, Virginia 22217

27 10 2 059

REPORT DOCUMENTATION PAGE

1a. REPORT SECURITY CLASSIFICATION UNCLASSIFIED			1b. RESTRICTIVE MARKINGS NONE		
2a. SECURITY CLASSIFICATION AUTHORITY			3. DISTRIBUTION/AVAILABILITY OF REPORT Approved for public release; distribution unlimited		
2b. DECLASSIFICATION/DOWNGRADING SCHEDULE					
4. PERFORMING ORGANIZATION REPORT NUMBER(S) 021779-3-T			5. MONITORING ORGANIZATION REPORT NUMBER(S)		
6a. NAME OF PERFORMING ORGANIZATION Communications & Signal Processing Laboratory		6b. OFFICE SYMBOL (If applicable)	7a. NAME OF MONITORING ORGANIZATION Office of Naval Research Code 1125UA		
6c. ADDRESS (City, State, and ZIP Code) The University of Michigan Ann Arbor, MI 48109			7b. ADDRESS (City, State, and ZIP Code) 800 North Quincy Street Arlington, Virginia 22217		
8a. NAME OF FUNDING/SPONSORING ORGANIZATION		8b. OFFICE SYMBOL (If applicable)	9. PROCUREMENT INSTRUMENT IDENTIFICATION NUMBER Contract No. N00014-84-K-0066		
8c. ADDRESS (City, State, and ZIP Code)			10. SOURCE OF FUNDING NUMBERS		
			PROGRAM ELEMENT NO.	PROJECT NO.	TASK NO.
11. TITLE (Include Security Classification) Quadrature-Quadrature Phase Shift Keying (U)					
12. PERSONAL AUTHOR(S) D. Saha					
13a. TYPE OF REPORT Tech. Report		13b. TIME COVERED FROM _____ TO _____		14. DATE OF REPORT (Year, Month, Day) September 1986	
15. PAGE COUNT 120					
16. SUPPLEMENTARY NOTATION					
17. COSATI CODES			18. SUBJECT TERMS (Continue on reverse if necessary and identify by block number) Binary Communications Bandwidth Efficiency Coherent Communications		
FIELD	GROUP	SUB-GROUP			
19. ABSTRACT (Continue on reverse if necessary and identify by block number) Quadrature-Quadrature phase shift keying (Q^2 PSK) is a new spectrally efficient modulation scheme which can be considered as two minimum shift keying type signalling schemes in parallel. It uses two data shaping pulses and two carriers which are pairwise quadrature in phase; the scheme thus utilizes available signal space dimensions in an efficient way to increase the bandwidth efficiency by a factor of two over two dimensional schemes such as QPSK, MSK, TFM. The bit error rate performance, however, depends on the choice of the data shaping pulse pair. With simple cosinusoidal and sinusoidal data shaping pulses the E_b/N_0 requirement is approximately 1.6 dB higher than that of MSK and 0.6 dB higher than that of TFM. With the suboptimum pulse shapes discussed in chapter six, the bit error rate performance of Q^2 PSK becomes closer to that of MSK, though for a given bandwidth the transmission rate in Q^2 PSK remains twice the rate in MSK.					
20. DISTRIBUTION/AVAILABILITY OF ABSTRACT <input checked="" type="checkbox"/> UNCLASSIFIED/UNLIMITED <input type="checkbox"/> SAME AS RPT <input type="checkbox"/> DTIC USERS			21. ABSTRACT SECURITY CLASSIFICATION UNCLASSIFIED		
22a. NAME OF RESPONSIBLE INDIVIDUAL Carol G. Van Aken			22b. TELEPHONE (Include Area Code) 313) 764-5210		22c. OFFICE SYMBOL



Debabrata Saha
All Rights Reserved

1986

To my parents and my teachers

ACKNOWLEDGEMENTS

I am sincerely grateful to Prof. Birdsall for his inspiration, guidance and assistance in preparing this dissertation. His readiness for discussion and, above all, his way of expressing problems in simple form contributed greatly towards this work. I am also indebted to Prof. Root for his valuable suggestions; his encouragement was a primary driving force behind initiating this work. I would like to thank members of my dissertation committee, Prof. Hero, Prof. Macnee and Prof. Stark for their criticisms and suggestions.

I am thankful to all the members of Cooley Electronics Laboratory for all the extensive facilities made available to me. In particular, John's assistance in programming and Carol's in administrative affairs are greatly appreciated. I take this opportunity to thank my friends and colleagues Fuad and Matt for their interest in my work; their good humor made the effort a pleasure. I also thank my friend Debashis for helping me on the word processor.

The partial support of the Office of Naval Research (code 1125) is also acknowledged.

Special thanks go to my brother Swapan, sister Protima and wife Namita for constant encouragements. Finally, I would like to express my deep gratitude towards my parents for their inspirations and sacrifices.

TABLE OF CONTENTS

DEDICATION	ii
ACKNOWLEDGEMENTS	iii
LIST OF TABLES	vi
LIST OF FIGURES	vii
LIST OF APPENDICES	ix
CHAPTER	
ONE. INTRODUCTION	1
TWO. CURRENT MODULATION TECHNIQUES	7
2.1. Quadrature Phase Shift Keying, Offset Quadrature Phase Shift Keying and Minimum Shift Keying	8
2.2. Tamed Frequency Modulation	11
2.3. Quadrature Overlapped Raised Cosine Signalling Scheme	15
2.4. Correlative Coding Technique	17
2.5. Summary	22
THREE. QUADRATURE-QUADRATURE PHASE SHIFT KEYING	23
3.1. Problem Background	23
3.2. Quadrature-Quadrature Phase Shift Keying	25
3.3. Energy Efficiency	29
3.4. Power Spectral Density and Effect of Bandlimiting	34
3.5. Modulator Demodulator and Synchronization Scheme	44
3.6. Summary	49
FOUR. QUADRATURE-QUADRATURE PHASE SHIFT KEYING: A CONSTANT ENVELOPE MODULATION SCHEME	50
4.1. Introduction	50
4.2. Constant Envelope Q ² PSK	51
4.3. Demodulation and Synchronization	55
4.4. Summary	59

FIVE.	GENERALIZED QUADRATURE-QUADRATURE PHASE SHIFT KEYING	60
	5.1. Introduction	60
	5.2. Formulation of Generalized Q^2 PSK	61
	5.3. Q^2 PSK ($n=3$)	64
	5.4. Spectral Density	68
	5.5. Summary	77
SIX.	PULSE SHAPING AND NYQUIST RATE	78
	6.1. Introduction	78
	6.2. Pulse Shaping	79
	6.3. Solutions to Pulse Shaping Problem	85
	6.4. Summary	88
SEVEN.	CONCLUDING REMARKS	89
	7.1. Thesis Summary	89
	7.2. Possible Future Developments	91
APPENDICES	94
REFERENCES	105

LIST OF TABLES

Table

3.1. Energy and Bandwidth Efficiencies of Q^2 PSK, Two and Four Level MSK	43
5.1. Energy and Bandwidth Efficiencies of MSK, Q^2 PSK and Generalized Q^2 PSK	75

LIST OF FIGURES

Figure	
2.1. Quadrature-Quadrature Phase Shift Keying modulator	9
2.2. Staggering of data pulses in OQPSK and MSK for the data stream $a_k(t)$ in Figure 2.1	9
2.3. Phase trajectories of (a) MSK and (b) TFM signals	12
2.4. Two different realizations of TFM signals	12
2.5. Duobinary signalling scheme. $H(f)$ is the equivalent frequency response of the cascade of digital filter and Nyquist's minimum bandwidth filter $G(f)$	20
2.6. Precoded Duobinary signalling scheme	20
3.1. Quadrature-Quadrature Phase Shift Keying (Q^2 PSK) modulator	27
3.2. Wave shaping of the data pulses in Q^2 PSK for the data stream $a_k(t)$ in Figure 3.1	27
3.3. Spectral densities of OQPSK, MSK and Q^2 PSK modulated signals	37
3.4. Percent power captured as function of bandwidth of MSK, QPSK and Q^2 PSK signals	37
3.5. Bit error probabilities as functions of E_b/N_0 for Q^2 PSK , QPSK and MSK signals	42
3.6. Realization of Q^2 PSK - modulator	45
3.7. Realization of Q^2 PSK - demodulator	45
3.8. Synchronization scheme for coherent demodulation of Q^2 PSK signal	47
4.1. Constant envelope Q^2 PSK - modulator	54
4.2. Bit error probabilities as functions of E_b/N_0 for coded Q^2 PSK ,MSK, and TFM signals	56
4.3. Synchronization scheme for coherent demodulation of constant envelope Q^2 PSK signal	56
5.1. Truncated Sinc function as data shaping components for Q^2 PSK ($n=3$)	66

5.2. Spectral densities of MSK signal and Q^2 PSK signals using (a) simple (b) composite and (c) Truncated Sinc function wave shapings	71
5.3. Percent power captured as function of bandwidth for MSK and Q^2 PSK ($n=3$) using truncated Sinc, Simple and Composite wave shapings	72
5.4. Bit error probabilities as functions of of E_b/N_0 for Q^2 PSK (simple wave shape), MSK and QORC signals	76
6.1. Baseband model of Q^2 PSK transmitter and receiver	81
6.2. Transmitter filter pairs for Q^2 PSK transmitter with zero inphase and zero cross intersymbol interference	86
B.1. Coding for four level MSK	100

LIST OF APPENDICES

Appendix

A. Probability Density Function of Signal Level in Bandlimited Situation	95
B. Q^2 PSK and Four Level MSK	99
C. Sufficient Statistic for Decision in Coded Q^2 PSK	103

CHAPTER ONE

INTRODUCTION

The continual increase in the demand for reliable communication through digital transmission calls for spectrally efficient modulation schemes. Spectrally efficient modulation, sometimes, in some loose sense, is referred to as the use of power to save bandwidth, much as coding is referred to as the use of bandwidth to save power. However, a meaningful measure of spectral efficiency lies in the notion of effective use of available signal space dimensions. The more effectively the available dimensions are used to increase the transmission throughput, the higher is the spectral efficiency. This notion of effective use of available signal space is the central idea of this thesis and leads to the development of a new class of digital modulation schemes which has been named Quadrature-Quadrature Phase Shift Keying or Q^2PSK .

The primary objective of a spectrally efficient modulation scheme is to maximize the bandwidth efficiency (b), defined as the ratio of data rate (R_b) to channel bandwidth (W). Since a signal cannot be both strictly duration-limited and strictly bandlimited, there are two approaches in designing a spectrally efficient data transmission scheme. One is the bandlimiting approach; the other is the timelimiting approach. In the former, a strictly bandlimited spectral shape is carefully chosen for the data pulse so as to satisfy the Nyquist criterion of zero

intersymbol interference (ISI). In the latter, the data pulse is designed to have a short duration and the definition of bandwidth is somewhat relative depending on the situation involved. The initial development of Q^2PSK followed the latter approach; the former approach, however, proved useful in the final stage.

Like bandwidth, power is also a costly resource in most transmission environments. So another objective in designing a high rate data transmission scheme is to reduce the average energy per bit (E_b) needed to achieve a specified bit error rate (BER). The bit error rate performance of two schemes are usually compared under the assumption of a bandlimited channel corrupted by additive white Gaussian noise (AWGN). Suppose the two sided power spectral density of the noise is $N_0/2$. Then a standard parameter for comparing the two modulation schemes is the energy efficiency which is the ratio E_b/N_0 required to achieve a specified bit error rate, say 10^{-5} ; the lower the energy efficiency, the better is the performance.

The energy efficiency depends mostly on the signal space geometry. The bandwidth efficiency primarily depends on two factors; firstly the basic waveforms of the data shaping pulses and secondly the utilization of all possible signal space dimensions available within the given transmission bandwidth. In data communication, the notion of increasing the rate of transmission by increasing the number of dimensions became prominent when people switched from Binary Phase Shift Keying (BPSK) to Quadrature Phase Shift Keying (QPSK). Modulation studies during the last twenty years proposed several modifications of QPSK. Of these, Offset Quadrature Phase Shift Keying (OQPSK) and Minimum

Shift Keying (MSK) gained popularity because of their several attributes. Numerous variations of QPSK and MSK have been reported in the literature; but almost all of them follow the same QPSK assumption of two dimensional transmission. Tamed Frequency Modulation (TFM) and relatively unknown Quadrature Overlapped Raised Cosine Modulation (QORC) followed slightly different approaches to attain a sharp spectrum fall-off for lower out-of-band radiation. Unfortunately, both of them introduce intersymbol interference (ISI) in the system and suffer from a loss in the energy efficiency over MSK. In the next chapter we will briefly review some of these schemes and point out their attributes and shortcomings.

Shannon's channel capacity theorem [1] provides an upper bound to the bandwidth efficiency for a given signal energy. It is observed that the order of bandwidth efficiency one achieves with the currently existing schemes is very poor compared to the maximum bandwidth efficiency allowed by Shannon's channel capacity bound. The large gap between Shannon's bound and practically achieved bandwidth efficiency may motivate someone to improve the bandwidth efficiency by a factor of five or more. However, if one restricts oneself to binary type of communication, an improvement by a factor of two can be expected [2]. It is well known that the space of signals essentially limited in time to an interval τ and in one sided bandwidth occupancy to W is essentially $2\tau W$ -dimensional. It is observed that the shortcomings of the existing schemes lie in the inefficient use of available signal space dimensions. For a given bandwidth equal to the data rate, QPSK and MSK use only as much as half of the available dimensions. In

chapter three we propose Quadrature-Quadrature Phase Shift Keying or Q^2PSK which utilizes all available signal space dimensions. It uses two data shaping pulses and two carriers, which are pairwise quadrature in phase, and creates two more dimensions in addition to the existing two already in use by QPSK and MSK. The new scheme thus increases the bandwidth efficiency by a factor of two over the conventional schemes without altering the average bit energy requirement substantially. One may recall that QPSK brought the same sort of improvement over BPSK; Q^2PSK does it again over QPSK and MSK.

Q^2PSK utilizes all available signal space dimensions; therefore incoherent detection is not possible at the receiver. For coherent detection, one needs to know the carrier phase and clock timing information. In certain transmission systems, such as partial response signalling schemes, this information can be carried out by separate pilot tones at the spectral nulls of the modulated signal. However, in most situations it is more desirable that one recovers this information from the modulated signal itself. It will be shown that Q^2PSK signal has self clocking and self synchronizing ability. In chapter three we present a synchronization scheme which recovers carrier phase and clock timing information.

In designing a modulation scheme, though energy and bandwidth efficiencies are the two most important criteria, a constant envelope in the modulated signal may be an additional desirable feature for certain nonlinear type of channels [3]. For instance, the travelling wave tube (TWT) amplifier in a satellite repeater usually converts amplitude variations to spurious phase modulation. This AM to PM conversion causes degradation in the bit error rate performance of the signal.

A constant envelope in the modulated signal may reduce this problem to a great extent. Also if the channel is nonlinear due to the presence of class C devices, a constant envelope may be an essential requirement. In both situations, MSK with its constant envelope does a very good job. Tamed Frequency Modulation (TFM) [4], which is another constant envelope scheme, is preferred to MSK in certain situations where low level out-of-band radiation is more important than a loss in the energy efficiency. The Q^2PSK signal, in the absence of any additional constraint, does not maintain a constant envelope. However, a simple block coding prior to modulation provides a constant envelope. This coded Q^2PSK outperforms TFM in both energy and bandwidth efficiencies. Its bandwidth efficiency is of the order of 1.5 times that of MSK and TFM. Like uncoded Q^2PSK , this coded scheme also possesses self clocking and self synchronizing ability; but the required synchronizing scheme is different from that of the uncoded version.

Q^2PSK uses two data shaping pulses and two carriers which are pairwise quadrature in phase. The scheme is generalized by incorporating n orthogonal data shaping pulses alongwith two orthogonal carriers to create a $2n$ -dimensional signal space. The bandwidth requirement in the formation of this signal space, however, increases with the number n . The original case of $n=2$ increases the bandwidth efficiency by a factor of two over MSK at the expence of 1.6 dB increase in the average bit energy. The extra bit energy requirement is avoided by allowing a loss in the bandwidth efficiency; in the special case of $n=3$, a bandwidth efficiency which is 1.5 times that of MSK is achieved without any increase in the average bit energy. This bandwidth efficiency is also 1.5 times

that of QORC [5], which is a non constant envelope scheme but more spectrally compact than MSK. This generalized Q^2PSK does not maintain a constant envelope; its spectral density, however, falls off faster than the original Q^2PSK .

The original Q^2PSK uses a half cosinusoid and a half sinusoid as two data shaping pulses. On bandlimiting, these two pulses cause intersymbol interference and therefore Q^2PSK requires a little higher bit energy compared to MSK. In an attempt to eliminate both in phase and cross intersymbol interference a new class of pulse shapes is suggested. A few members of this class are easily implementable and improve both energy and bandwidth efficiencies considerably over the original scheme. This new class of pulse shapes also sheds some light on an important issue of binary communication. It is well known that the best rate one can achieve with binary communication is the Nyquist rate of two bits per second per Hertz; this is only possible if one uses a sinc function as the data shaping pulse. But realization of a sinc function is known to have problems from both theoretical and implementation points of view. One solution was given by Adam Lender through his Duobinary scheme [6]. We will briefly discuss the Duobinary scheme in the next chapter. The Duobinary signal achieves the Nyquist rate but it does not maintain a binary type of communication; it uses three level detection. The new class of pulse shapes that we will propose in chapter six requires less bit energy and achieves the Duobinary rate with only two level detection.

CHAPTER TWO

CURRENT MODULATION TECHNIQUES

On off Keying is the most primitive digital modulation scheme which uses two states of a signal to represent binary zeros and ones. In Binary Phase Shift Keying (BPSK), these two states are represented by two opposite phases of a carrier; this is an antipodal signalling scheme. Quadrature Phase Shift Keying (QPSK) can be considered as two BPSK systems in parallel; it uses two orthogonal carriers of the same frequency for the two BPSK systems. QPSK transmission is thus two dimensional. Many of the current modulation schemes maintain the basic QPSK-assumption of two dimensional transmission. In this chapter we will discuss some of current modulation techniques which follow the two dimensional assumption in a direct or indirect sense. Namely, we will discuss Quadrature Phase Shift Keying (QPSK), Offset Quadrature Phase Shift Keying (OQPSK), Minimum Shift Keying (MSK), Quadrature Overlapped Raised Cosine (QORC) signalling scheme, Tamed Frequency Modulation (TFM) and Duobinary scheme. Some of the schemes maintain constant envelope, some of them do not; we consider both types of modulation for evaluating Q^2PSK performance in different perspectives.

2.1 Quadrature Phase Shift Keying, Offset Quadrature Phase Shift Keying and Minimum Shift Keying

A block diagram of the *QPSK* modulation scheme [3,7] is shown in Figure 2.1. The input binary data stream $a(t)$ with the bit rate $1/T$ is demultiplexed into two streams $a_1(t)$ and $a_2(t)$. The duration of each bit in the demultiplexed streams is twice the duration of the incoming bit. Streams $a_1(t)$ and $a_2(t)$ are multiplied by sine and cosine carriers and summed to form the *QPSK* signal $s_{qpsk}(t)$.

$$\begin{aligned} s_{qpsk}(t) &= \frac{1}{\sqrt{2T}} a_1(t) \cos(2\pi f_c t + \frac{\pi}{4}) + \frac{1}{\sqrt{2T}} a_2(t) \sin(2\pi f_c t + \frac{\pi}{4}) \\ &= \frac{1}{\sqrt{T}} \cos(2\pi f_c t + \phi(t)) \end{aligned} \quad (2.1)$$

where each of $a_1(t)$ and $a_2(t)$ is either +1 or -1 and $\phi(t)$, depending on $a_1(t)$ and $a_2(t)$, is one of 0° , $\pm 90^\circ$ and 180° . Thus carrier phase during any $2T$ interval is one of the four phases. In the next $2T$ interval, if neither of the two bit streams changes sign, the carrier phase remains the same. If one of them changes sign, a phase shift of $\pm 90^\circ$ occurs. A change of sign in both streams causes a phase shift of 180° . Rapid changes in the carrier phase has deteriorating effects on the signal and the adjacent channel when it undergoes bandlimiting and hardlimiting operations.

These deteriorating effects are partially eliminated in Offset Quadrature Phase Shift Keying (*OQPSK*) [3,7] where the two bit streams are not allowed to change their sign simultaneously, thus avoiding the possibility of 180° phase shift. This is accomplished by skewing or delaying the bit stream $a_2(t)$ by an

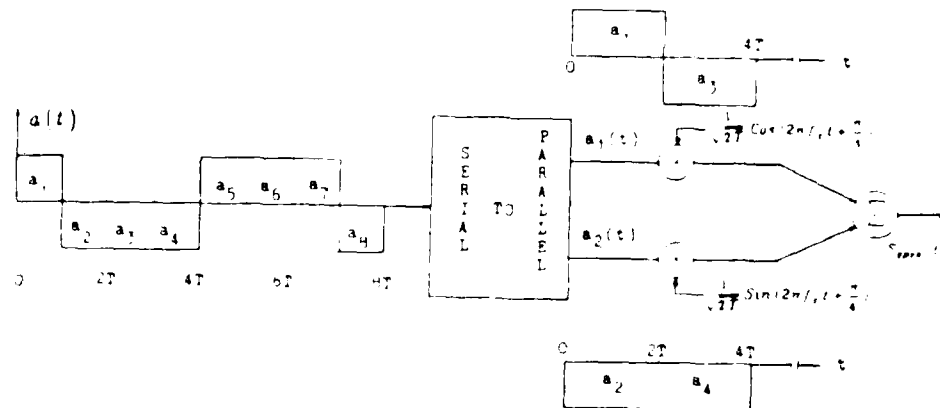


Figure 2.1. Quadrature Phase Shift Keying modulator.

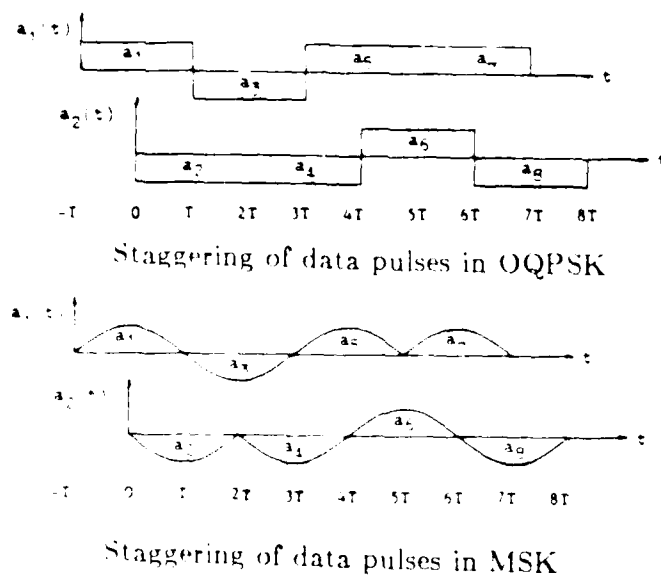


Figure 2.2. Staggering of data pulses in OQPSK and MSK for the data stream $a_k(t)$ in Figure 2.1.

amount of time T as illustrated in Figure 2.2. By pulse shaping, further elimination of abrupt changes in the carrier phase is possible. In fact, it is totally eliminated in Minimum Shift Keying (*MSK*) [3,8,9] where a cosinusoidal data shaping pulse is used in place of the rectangular one of *OQPSK*, as illustrated in Figure 2.2. This pulse shaping in *MSK* also brings some spectral compactness over *OQPSK*. The *MSK* signal can be written as

$$\begin{aligned} s_{msk}(t) &= \frac{1}{\sqrt{T}} a_1(t) \cos\left(\frac{\pi t}{2T}\right) \cos(2\pi f_c t) + \frac{1}{\sqrt{T}} a_2(t) \sin\left(\frac{\pi t}{2T}\right) \sin(2\pi f_c t) \\ &= \frac{1}{\sqrt{T}} \cos\left[2\pi\left(f_c + \frac{b(t)}{4T}\right)t + \phi(t)\right] \end{aligned} \quad (2.2)$$

where $b(t) = -a_1(t)a_2(t)$, and $\phi(t) = 0$ or π according to $a_1 = +1$ or -1 . Thus *MSK* signals can have one of two instantaneous frequencies, $f_c \pm \frac{1}{4T}$. The spacing between the two frequencies is $\frac{1}{2T}$. This is the minimum spacing with which two *FSK* signals of duration T can be orthogonal; hence the name Minimum Shift Keying (*MSK*). The baseband power spectral densities $S_{qpsk}(f)$ and S_{msk} for *QPSK* (or *OQPSK*) and *MSK* are given by

$$\frac{1}{T} S_{qpsk}(f) = 2 \left[\frac{\sin 2\pi f T}{2\pi f T} \right]^2 \quad (2.3)$$

$$\frac{1}{T} S_{msk}(f) = \left[\frac{16}{\pi^2} \right] \left[\frac{\cos 2\pi f T}{1 - 16f^2 T^2} \right]^2 \quad (2.4)$$

where in all cases,

$$\int_{-\infty}^{\infty} S(f) df = 1. \quad (2.5)$$

In chapter three we will discuss these spectra along with that of Quadrature-Quadrature Phase Shift Keying

2.2 Tamed Frequency Modulation

TFM is a type of frequency modulation [4,10] suitable for digital transmission. We know frequency modulation is different from frequency shift keying; in the former frequency transitions are smooth, in the latter frequency transitions are abrupt. The difference, therefore, lies in the phase trajectories of the carrier or central frequency. So in considering TFM in a group of modulation schemes most of which are frequency shift keying types, phase trajectory turns out to be a common ground for discussion. We would like to pursue the discussion of TFM on this ground. One may consider TFM as an improvement in the phase trajectories of MSK with the use of correlative coding; in that sense, TFM also follows the basic QPSK assumption of two dimensional transmission.

We mentioned earlier that MSK uses one of the two frequencies $f^+ = (f_c + 1/4T)$ and $f^- = (f_c - 1/4T)$ to represent the demultiplexed bit streams (Figure 2.1) over every bit interval of T . So another way of representing an MSK signal is the following : instead of demultiplexing the input bit streams and then representing them by one of the two frequencies, one may directly represent a $+1$ by f^+ and a -1 by f^- such that phase is continuous at the bit transition instants. The excess phase of the carrier of frequency f_c is given by

$$\phi_k(t) = a_k \frac{\pi t}{2T} \quad (2.6)$$

A typical phase trajectory of MSK signal (Figure 2.3) shows frequent slope discontinuities. The spectral density of MSK would have been narrower if the

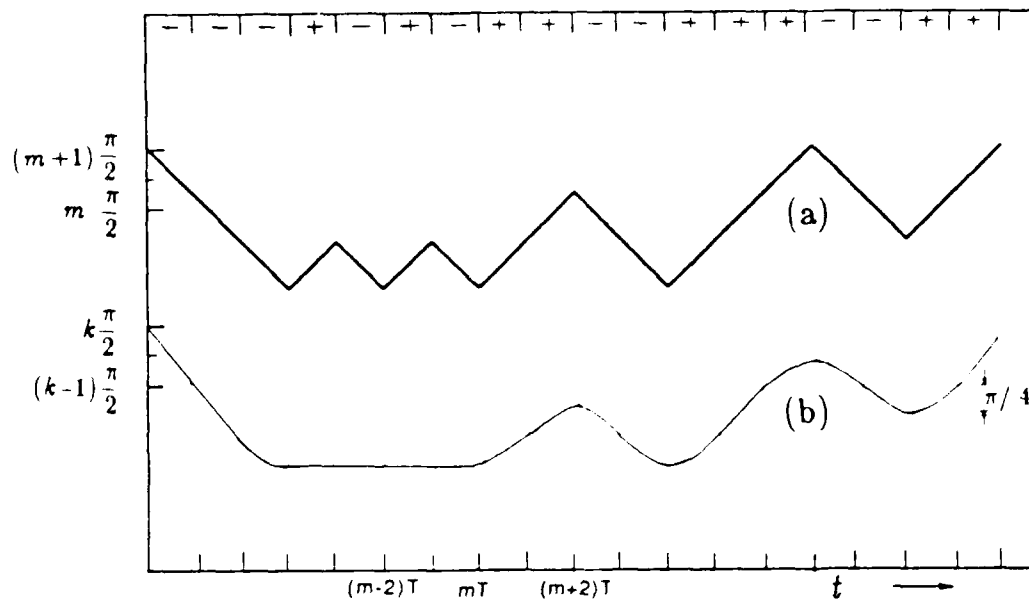


Figure 2.3. Phase trajectories of (a) MSK and (b) TFM signals.

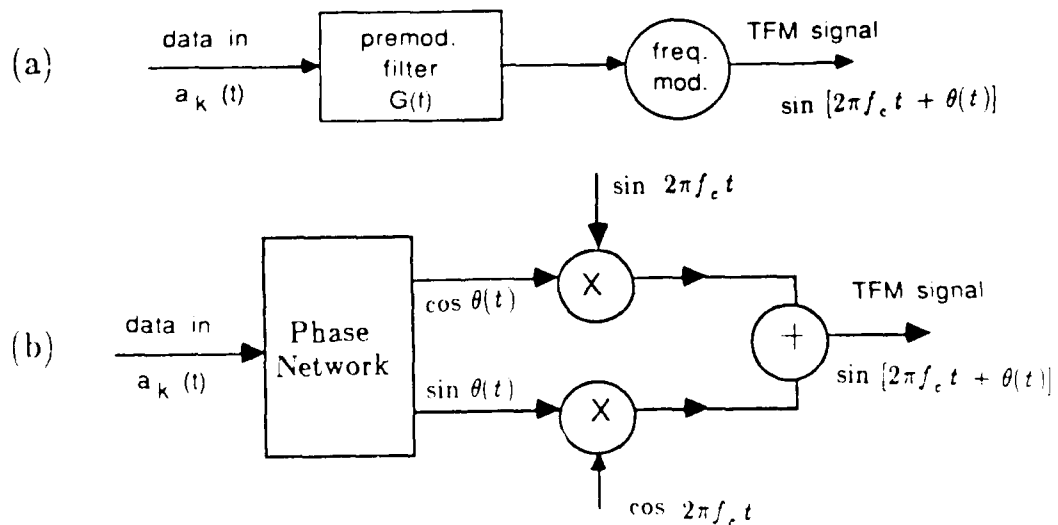


Figure 2.4. Two different realizations of TFM signals.

edges of the phase path were smoothed out. In an attempt to achieve higher spectral compactness, TFM uses correlative coding for smoothing out oscillations and sharp edges of the phase path. A typical TFM phase trajectory is also shown in Figure 2.3. For MSK,

$$\theta(nT + T) - \theta(nT) = (\pi/2) \cdot a_n \quad (2.7)$$

and for TFM,

$$\theta(nT + T) - \theta(nT) = (\pi/2) \cdot \left(\frac{a_{n-1}}{4} + \frac{a_n}{2} + \frac{a_{n+1}}{4} \right) \quad (2.8)$$

with $\theta(0) = 0$ if $a_0, a_1 = 1$ and $\theta(0) = \pi/4$ if $a_0, a_1 = -1$. In addition to going through the phase values given by (2.8) the phase variation should be as smooth as possible, as shown in Figure 2.3b. From the coding rule illustrated in (2.8) it follows that phase changes of $\frac{\pi}{2}$ are obtained if three consecutive bits have the same polarity, and the phase remains constant if the three bits are of alternating polarity. Phase changes of $\frac{\pi}{4}$ occur when the bit configuration is one of $+-$, $-++$, $++-$, $--+$.

Two different block diagrams of a TFM modulator are shown in Figure 2.4: Figure 2.4a describes TFM as frequency modulation while Figure 2.4b focusses the two dimensional nature of transmission. The impulse response $g(t)$ of the premodulation filter $G(f)$ in Figure 2.4a is such that the phase function $\theta(t)$ of the frequency modulated signal satisfies (2.8). One can show that the overall transfer function of the premodulation filter can be written as

$$G(f) = K H(f) \cos^2 \pi f T \quad (2.9)$$

where K is a constant and $H(f)$ is any transfer function whose impulse response $h(t)$ satisfies the third Nyquist criterion. This criterion states that for any integer k :

$$\begin{aligned} \int_{(2k-1)T/2}^{(2k+1)T/2} h(t) dt &= 1 & k &= 0 \\ &= 0 & k &\neq 0 \end{aligned} \quad (2.10)$$

A minimum bandwidth choice for $H(f)$ is

$$\begin{aligned} H(f) &= \frac{\pi f T}{\sin \pi f T} & w &\leq 1/2T \\ &= 0 & w &> 1/2T \end{aligned} \quad (2.11)$$

With this choice of $H(f)$, an approximate expression for bit error probability of TFM [4] is given by

$$P_{b \text{ TFM}}(E) = \frac{1}{2} Q(\sqrt{2\bar{E}_b/N_0}) + \frac{1}{2} Q(\sqrt{1.4\bar{E}_b/N_0}) \quad (2.12)$$

Similarly for MSK,

$$P_{b \text{ MSK}}(E) = Q(\sqrt{2\bar{E}_b/N_0}) \quad (2.13)$$

where

$$Q(u) = \frac{1}{\sqrt{2\pi}} \int_u^{\infty} \exp(-x^2/2) dx \quad (2.14)$$

The spectral density of TFM signal depends considerably on the truncation length of the impulse response of the premodulation filter; there is no closed form expression for the spectral density. However, if the truncation length is of the order of $7T$ or more, substantial improvement in the out-of-band radiation is observed [4]. The correlative coding used in constructing the TFM signal has two

fold effects : (i) it smoothes out the phase trajectories of the carrier; as a result, out-of-band radiation is substantially lower compared to other constant envelope modulation schemes such as MSK, (ii) it introduces more than two levels (unlike MSK) at the demodulator output [4]; the levels are ± 1 , ± 0.707 . As a result, the bit error rate performance is poorer; it suffers a 1 dB loss in the energy efficiency over MSK at bit error rate of 10^{-5} . TFM is considered to be a better candidate than MSK where bandlimiting filtering is costly and low level out of band radiation is more important than a loss in the energy efficiency.

2.3 Quadrature Overlapped Raised Cosine Signalling Scheme

Any two dimensional modulated bandpass signal such as QPSK and MSK signals can be written as

$$s(t) = a_1(t) p(t) \cos 2\pi f_c t + a_2(t) p(t) \sin 2\pi f_c t \quad (2.15)$$

where $a_1(t)$ and $a_2(t)$ are the demultiplexed bit streams and $p(t)$ is the pulse shaping component. For QPSK,

$$\begin{aligned} p(t) = q(t) &= \frac{1}{\sqrt{2T}} & t \in [-T, T] \\ &= 0 & t \in [-T, T] \end{aligned} \quad (2.16a)$$

and for MSK (except for a relative time offset of T),

$$\begin{aligned} p(t) = m(t) &= \sqrt{\frac{T}{T}} \cos \left(\frac{\pi t}{2T} \right) & t \in [-T, T] \\ &= 0 & t \in [-T, T] \end{aligned} \quad (2.16b)$$

Both QPSK and MSK are constant envelope modulation schemes; their spectral densities fall off as f^{-2} and f^{-4} respectively. A third kind of two dimensional non constant envelope scheme can be described by a pulse shaping component which is the convolution of the pulse shapes in (2.16a) and (2.16b) and given by

$$\begin{aligned} p(t) = h(t) &= A \, q(t+T) \otimes m(t+T) \\ &= \frac{1}{\sqrt{6T}} \left(1 + \cos \frac{\pi t}{T} \right) \quad |t| \leq 2T \\ &= 0 \quad |t| > 2T, \quad (2.17) \end{aligned}$$

where A is a normalizing constant (a function of T) so that $p(t)$ is a unit energy pulse and \otimes denotes time convolution. Here $h(t)$ is a raised cosine pulse which extends from $-2T$ to $+2T$, and therefore causes overlapping with the adjacent pulses on either side; hence the name is Quadrature Overlapped Raised Cosine (QORC) signalling scheme [5]. Its power spectral density is the product of QPSK and MSK spectral densities and therefore falls off as f^{-6} . The spectral density is given by

$$S_{qorc}(f) = \frac{2T}{3} \left(\frac{\sin 4\pi f T}{2\pi f T (1-16f^2 T^2)} \right)^2. \quad (2.18)$$

In addition to f^{-6} spectral fall off, QORC retains the same first null as QPSK (the first null of MSK is at 1.5 times that of QPSK). QORC is more spectrally compact than MSK and QPSK, but it does not maintain a constant envelope. Because of the overlapping of adjacent pulses, matched filter detection is not optimum; detections with QPSK and MSK demodulators are two possibilities. In spite of its non constant envelope, QORC has been reported [5] to outperform MSK in certain nonlinear channels.

2.4 Correlative Coding Technique

All schemes we have discussed so far in this chapter use short duration pulses to represent binary zeros and ones; the duration of the pulse is of the order of the signalling interval. One may call this the time limited approach. In this approach the spectral density is not expected to be strictly bandlimited; it falls off asymptotically as some power of frequency f . In contrast, however, there lies another approach namely, the bandlimited approach; this is mostly due to Nyquist. Nyquist [2] considered the problem of designing a pulse shape $p(t)$ which is strictly bandlimited and causes no intersymbol interference (ISI) at regular sampling instants nT , where T is the signalling interval. He showed that the minimum bandwidth required to transmit R bits/second (or R symbols/second when one considers nonbinary transmission) is $R/2$ Hz ; the corresponding pulse shape is a sinc function given by

$$p(t) = \frac{\sin \pi R t}{\pi R t} . \quad (2.19)$$

The pulse $p(t)$ has long tails, but the tails pass through zeros at regular sampling instants of $t = n/R$ sec, where n is a nonzero integer, thus creating no interference with adjacent symbols. So the maximum rate at which one can transmit binary data is 2 bits/second Hz; this is called the " Nyquist Rate ".

Unfortunately, the pulse of (2.19) is theoretically impossible to achieve without an infinite delay. Also, any approximation of it with finite delay is impractical because its slowly varying tail causes considerable intersymbol interference if there is even a small time jittering in the sampler. The slow decay

of the tail is due to the discontinuity in the spectrum at the band edge. Nyquist also considered more practical shapes with smooth transition at the band edge. But all these filter shapes require a bandwidth in excess of $R/2$ Hz. One frequently used shape is the Raised Cosine Spectrum (which is different from QORC pulse in the time domain) with one hundred percent excess bandwidth. This yields a rate of one bit/second. Thus even though the maximum theoretical limit on efficiency set by Nyquist is two bits/second/Hz, the practical limit may lie close to one bit/second.

It should be noted that a key factor behind Nyquist's result is the assumption of zero memory modulation; the amplitudes of the pulses at respective sampling instants are independent of the adjacent pulses. In a finite memory modulation, the amplitude of the modulated signal at any sampling instant depends on a finite number of adjacent symbols. If one is willing to deal with such finite memory, Nyquist's rule of maximum theoretical limit does not apply [6,11]. A correlation among adjacent data pulses introduces some memory into the modulated signal. In an attempt to achieve the Nyquist rate, one may make use of this memory to relax the restrictions on the spectral sharpness of the Nyquist's minimum bandwidth filter.

Lender proposed such a correlative scheme, which is named Duobinary. The Duobinary scheme is considered as a practical means of achieving Nyquist's theoretical limit using realizable filters. However, it involves three level detection and therefore suffers a three dB loss in the energy efficiency over Nyquist's postulation. In chapter six we will propose a scheme which maintains binary type

communication and achieves the Nyquist rate with the use of easy realizable filters; the scheme is more energy efficient than Duobinary.

Duobinary scheme

Assume that a stream of binary sequence $\{ x_k \}$ is to be transmitted at the rate of R bits/sec over the Nyquist's minimum bandwidth ideal lowpass channel of bandwidth $R/2$ Hz. Let the bits be first passed through a simple digital filter followed by Nyquist's minimum bandwidth filter of frequency response $G(f)$ as shown in Figure 2.5. The effect of the digital filter is to add to the present bit of information the previous bit value. The symbol sequence $\{ y_k \}$ at the channel input is

$$y_k = x_k + x_{k-1} . \quad (2.20)$$

The channel input amplitudes no longer remain independent. Every bit of information will interfere with the next bit. But this interference should be distinguished from the interference due to bandlimiting. The interference due to the digital filter is a controlled amount. This controlled amount of interference is the key difference between a correlative or partial response signalling system and a zero memory system as postulated by Nyquist. The equivalent frequency response of the cascade of the digital filter and the Nyquist's minimum bandwidth filter, $G(f)$, has transfer function

$$\begin{aligned} H(f) &= G(f) (1 + e^{-j2\pi f T}) \\ &= e^{-j\pi f T} \cdot 2G(f) \cdot \cos\pi f T . \end{aligned} \quad (2.21)$$

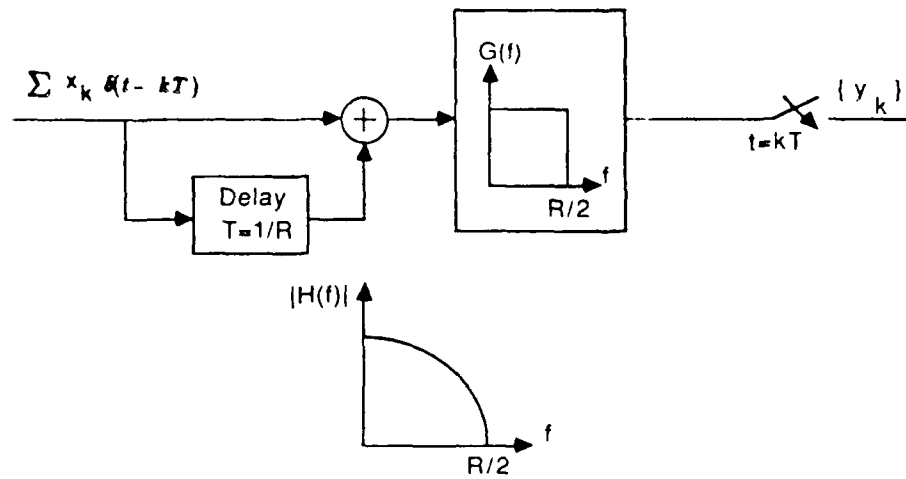


Figure 2.5. Duobinary signalling scheme. $H(f)$ is the equivalent frequency response of the cascade of digital filter and Nyquist's minimum bandwidth filter $G(f)$.

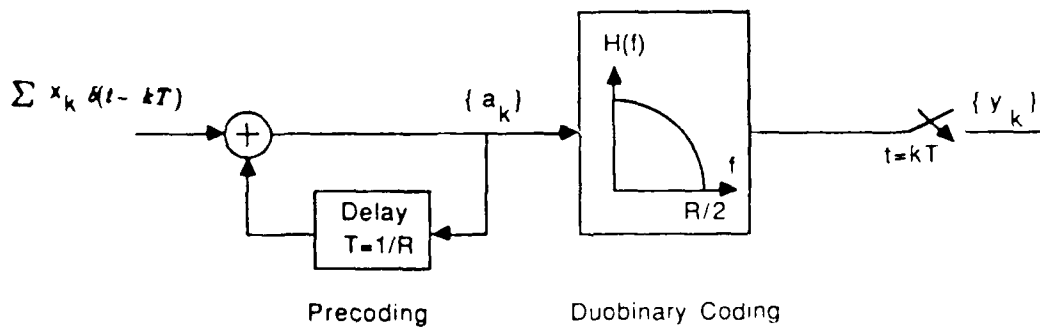


Figure 2.6. Precoded Duobinary signalling scheme

Thus $H(f)$ has a gradual roll-off to the band edge and it might be implemented by a practical and realizable analog filter. A separate digital filter is not required. The bandwidth requirement of $H(f)$ is no more than that of Nyquist's minimum bandwidth of $R/2$ Hz [11,12]. Thus Nyquist's rate is achieved; but as we will see shortly, this is at the expense of higher bit energy.

If x_k is ± 1 , then the channel input can be one of the three values: $-2, 0, +2$. Thus the binary input is converted into three level output. This three level detection requires about 3dB more signal energy than binary detection for the same error rate. The decision of x_k is based on the value of $(y_k - x_{k-1})$. An obvious drawback of this decision process is the error propagation; once an error is made, it tends to propagate. This error propagation can be avoided by a non-linear precoding technique due to Lender.

Precoding on input sequence

Let the input binary sequence $\{ x_k \}$ have values 0 and 1 and this sequence is converted into another binary sequence $\{ a_k \}$ such that

$$a_k = x_k \oplus a_{k-1} \quad (2.22)$$

where \oplus stands for modulo two addition. The 0,1 sequence $\{ a_k \}$ is then converted into a $-1, +1$ sequence $\{ b_k \}$ as

$$b_k = 2 a_k - 1. \quad (2.23)$$

The sequence is fed at the input of combined channel filter $H(f)$ as shown in Figure 2.6. At the output we get

$$y_k = b_k + b_{k+1} . \quad (2.24)$$

Using (2.22), (2.23) and (2.24) one can show that the decoding of x_k can be done as follows :

$$x_k = 0 \quad \text{if } y_k = \pm 2 , \quad (2.25a)$$

$$x_k = 1 \quad \text{if } y_k = 0 . \quad (2.25b)$$

Since no symbol other than y_k is involved in the decision of x_k , error propagation cannot occur.

2.5 Summary

The best rate that one can achieve through binary communication is the Nyquist's rate of two bits per second per Hz. A practical way of achieving this rate is the Duobinary scheme; the scheme, however, does not maintain binary type of communication; it needs three level detection. The duration of Duobinary data pulse is long compared to the signalling interval. Minimum Shift Keying (MSK) and Tamed Frequency Modulation (TFM) are two other popular signalling schemes which use relatively short duration data pulses. The rates they achieve are of the order of half the Nyquist's rate. Both of them maintain constant envelope which is a desirable feature for nonlinear type of channels. TFM is preferred to MSK in situations where bandlimiting filtering is costly and relatively lower level out of band radiation is more important than a loss in the energy efficiency.

CHAPTER THREE

QUADRATURE - QUADRATURE PHASE SHIFT KEYING

3.1 Problem Background

Binary Phase Shift Keying is an antipodal signalling scheme; its signal space geometry is one dimensional. Quadrature Phase Shift Keying can be considered as two BPSK systems in parallel; one with a sine carrier, the other with a cosine carrier of the same frequency. QPSK signal space is thus two dimensional. The increase in dimensions in QPSK without altering the transmission bandwidth increases the bandwidth efficiency by a factor of two over BPSK. Spectral compactness is further enhanced in MSK by using a cosinusoidal data shaping pulse instead of the rectangular one of QPSK. Though MSK and QPSK use different data shaping pulses, their signal space geometries are the same. Both of them use a set of four biorthogonal signals. The spectral compactness achieved in MSK over QPSK should be distinguished from the compactness achieved in QPSK over BPSK. In the former compactness comes from the shaping of the data pulse, while in the latter it comes from increasing the dimension within the given transmission bandwidth.

To see the possibility of any further increase in dimension without increasing the transmission bandwidth substantially, one has to look into the

time-bandwidth product. It is well known that the space of signals essentially limited in time to an interval τ and in one sided bandwidth occupancy to W is essentially $2\tau W$ -dimensional. Though this bound on dimensions is true for the best choice of orthonormal set, the prolate spheroidal wave functions [13], yet it justifies the reasoning behind any search for higher dimensional signal sets to achieve higher bandwidth efficiency. In both QPSK and MSK, signal duration τ is $2T$, where T is the bit interval in the incoming data stream. Suppose the channel is strictly bandlimited to $1/2T$ on either side of the carrier, i.e. one sided bandwidth occupancy is $W = 1/T$. With such a bandlimited channel a QPSK system will be able to transmit only ninety percent of its total power while an MSK system transmits ninety seven percent. The number of dimensions available within this bandwidth $W = \frac{1}{T}$ is $2\tau W = 4$. It is surprising that only two of them are utilized in QPSK and MSK. The remaining two are unrealized potentials. So one could hope for a modulation scheme with a bandwidth efficiency as much as twice that of QPSK or MSK. Prolate spheroidal wave functions are not practical. However, even if they were practical, expectation of one hundred percent increase in bandwidth efficiency will be too much. Yet the extra two dimensions give some room for improving the bandwidth efficiency by increasing the dimensionality of the signal space. Quadrature-Quadrature Phase Shift Keying [14,15,16] makes use of these additional dimensions and increases the bandwidth efficiency by a factor of two over the two dimensional schemes discussed in the previous chapter.

3.2 Quadrature - Quadrature Phase Shift Keying

Consider the following basis signal set :

$$s_1(t) = \cos(\pi t/2T) \cos 2\pi f_c t \quad , \quad |t| \leq T \quad (3.1a)$$

$$s_2(t) = \sin(\pi t/2T) \cos 2\pi f_c t \quad , \quad |t| \leq T \quad (3.1b)$$

$$s_3(t) = \cos(\pi t/2T) \sin 2\pi f_c t \quad , \quad |t| \leq T \quad (3.1c)$$

$$s_4(t) = \sin(\pi t/2T) \sin 2\pi f_c t \quad , \quad |t| \leq T \quad (3.1d)$$

$$s_i(t) = 0 \quad , \quad i = 1,2,3,4 \quad , \quad |t| > T \quad , \quad (3.1e)$$

and identify

$$\begin{aligned} p_1(t) &= \cos(\pi t/2T) \quad , \quad |t| \leq T \\ &= 0 \quad , \quad |t| > T \end{aligned} \quad (3.2a)$$

and

$$\begin{aligned} p_2(t) &= \sin(\pi t/2T) \quad , \quad |t| \leq T \\ &= 0 \quad , \quad |t| > T. \end{aligned} \quad (3.2b)$$

Later $p_1(t)$ and $p_2(t)$, which are quadrature in phase, will be identified as data shaping pulses, and sine and cosine functions of frequency f_c as carriers. It is to be noted that between any two signals in the set $\{s_i(t)\}$, there is a common factor which is either a data shaping pulse or a carrier component; the remaining factor in one is in quadrature with respect to the remaining factor in the other. This makes $\{s_i(t)\}$ a set of four equal-energy orthogonal signals under the restriction

$$f_c = n/4T \quad , \quad n = \text{integer} \geq 2 \quad (3.3)$$

The orthogonality remains invariant under the translation of the time origin by

multiples of $2T$, the duration of each signal. In other words, if $\{s_i(t)\}$ is defined by (3.1a) through (3.1d) for all t , then one will get orthogonality over every interval of $2T$ centered around $t = 2mT$, m being an integer.

The orthogonality of $\{s_i(t-2mT)\}$ suggests a modulation scheme, a schematic diagram of which is shown in Figure 3.1. Data from an IID binary (± 1) source at a rate $2/T$ is demultiplexed into four streams $\{a_i(t)\}$; duration of each data pulse (rectangular shaped with strengths ± 1) in the demultiplexed streams being $2T$. Each data stream $a_i(t)$ is multiplied by the output $s_i(t)$ of a signal generator which continuously emits $s_i(t)$, defined over all t . The product signals are summed to form the modulated signal $s(t)$.

At the receiver, four identical coherent generators are available. Then one may use the orthogonality of $\{s_i(t-2mT)\}$ to separate out the four data streams. In the presence of additive white Gaussian noise, a correlation receiver will perform this process of demodulation in the optimum sense of minimum probability of error.

The modulating signal $s_i(t)$ has two effects on the bit streams $a_i(t)$: one is the wave shaping of the data pulse; the other is the translation of the baseband spectrum to a bandpass region. Shaping of the data pulses is illustrated in Figure 3.2. It is to be noted that the two pulse trains associated with either carrier are orthogonal over any interval of duration $2T$ centered around $2mT$. This makes sense because the dimensionality of the signal set used in this scheme is four; two of them come from the orthogonality of the carriers, the remaining

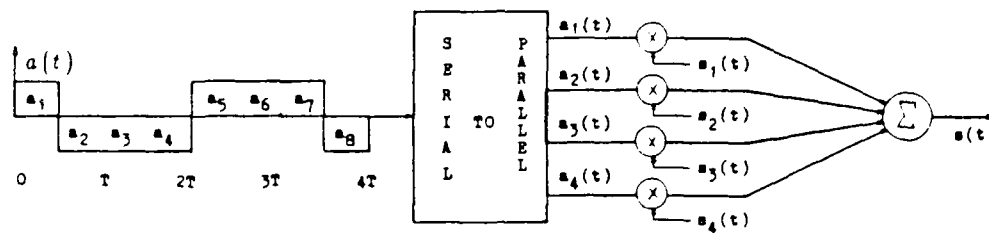


Figure 3.1. Quadrature-Quadrature Phase Shift Keying (Q^2PSK) modulator.

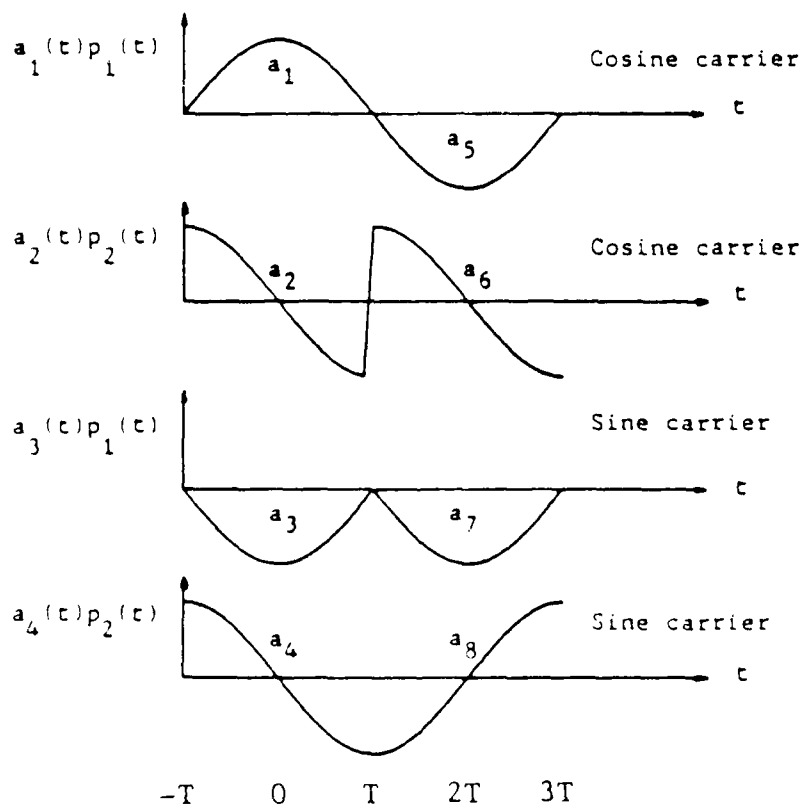


Figure 3.2. Wave shaping of the data pulses in Q^2PSK for the data stream $a_k(t)$ in Figure 3.1.

two from the orthogonality of the data shaping pulses $p_1(t)$ and $p_2(t)$. In other words, two carriers and two data shaping pulses are pairwise quadrature in phase. Hence the modulation scheme is named Quadrature - Quadrature Phase Shift Keying (Q^2PSK).

The bit rate $R_b = \frac{2}{T}$ at the input of the modulator in Figure 3.1 is twice the bit rate we considered for $QPSK$ and MSK schemes in the last section. This increase in the rate of transmission is due to the increase in the signal space dimensions. As conjectured earlier, this will result in a substantial increase in the bandwidth efficiency. For a quantitative comparison of the bandwidth efficiencies of Q^2PSK and MSK one needs to know the spectral occupancy of the Q^2PSK signal. We will discuss it shortly.

From Figure 3.1, one can represent the Q^2PSK signal as

$$s_{Q^2PSK}(t) = a_1(t) \cos\left(\frac{\pi t}{2T}\right) \cos(2\pi f_c t) + a_2(t) \sin\left(\frac{\pi t}{2T}\right) \cos(2\pi f_c t) + a_3(t) \cos\left(\frac{\pi t}{2T}\right) \sin(2\pi f_c t) + a_4(t) \sin\left(\frac{\pi t}{2T}\right) \sin(2\pi f_c t) \quad (3.4a)$$

$$= \cos[2\pi(f_c + b_{14}(t)/4T)t + \phi_{14}(t)] + \sin[2\pi(f_c + b_{23}(t)/4T)t + \phi_{23}(t)] \quad (3.4b)$$

where

$$b_{14}(t) = -a_1(t)a_4(t) \quad (3.5a)$$

$$\phi_{14}(t) = 0 \text{ or } \pi \text{ according as } a_1(t) = +1 \text{ or } -1 \quad (3.5b)$$

and

$$b_{23}(t) = -a_2(t)a_3(t) \quad (3.6a)$$

$$\phi_{23}(t) = 0 \text{ or } \pi \text{ according as } a_2(t) = +1 \text{ or } -1 \quad (3.6b)$$

Thus at any instant the Q^2PSK signal can be analyzed as consisting of two signals; one is cosinusoidal with frequency either of $(f_c \pm 1/4T)$, the other is sinusoidal with frequency either of $(f_c \pm 1/4T)$. The separation between the two frequencies associated with either of the two signals is $1/2T$; this is the minimum spacing that one needs for coherent orthogonality of two FSK signals as in MSK [3,14]. Comparison of (3.4b) with (2.2) shows that the cosinusoidal part of Q^2PSK signal in (3.4b) exactly represents an MSK signal. Therefore the Q^2PSK signalling scheme can be thought of as consisting of two minimum shift keying type signalling schemes, which, in some sense, are in quadrature with respect to each other. Since the two schemes are in quadrature, one can intuitively think that the overall energy efficiency will be the same as that of conventional MSK with half cosinusoid as data shaping pulse. Next we discuss the energy efficiency.

3.3 Energy Efficiency

An ultimate objective of all data communication systems is to reduce the bit error rate (BER) at the expense of a minimum amount of average bit energy (E_b). In practice, BER performance is usually evaluated under the assumption of a bandlimited channel corrupted by additive white Gaussian noise. In the following discussion, however, we do not consider the effect of bandlimiting; we consider the ideal signal space geometry. Let $N_0/2$ be the two-sided spectral density of the Gaussian noise. The receiver is assumed to be an optimum one, e.g. a correlation receiver, which maximizes the probability of correct decision. A

standard quantitative parameter for measuring *BER* performance is the energy efficiency; it is the ratio E_b/N_0 required to achieve a *BER* $P_b(E) = 10^{-6}$.

The signal set $\{s_i(t)\}$ used in Q^2PSK is of dimension $N = 4$. Each $s_i(t)$ represents one of four co-ordinate axes. With respect to this set of axes, a Q^2PSK signal can be represented as

$$s(t) = [a_1(t), a_2(t), a_3(t), a_4(t)] \quad (3.7)$$

where the coordinates $a_i(t)$'s can have only one of two values ± 1 with probability one half. The number of signals in the Q^2PSK signal set is 2^4 . The signals are equally probable and of equal energy, say E_s . The signal space geometry is the vertices of a hyper cube of dimension $N=4$; the centre of the cube being at the origin of the coordinate axes. For this signal space geometry, the signal error probability for any N [17,18], is given by

$$P_s(E) = 1 - (1-p)^N \quad (3.8)$$

where

$$p = Q(\sqrt{E_s/2N_0}) \quad (3.9a)$$

and

$$Q(v) = \frac{1}{\sqrt{1/2\pi}} \int_v^{\infty} \exp(-x^2/2) dx \quad (3.9b)$$

Signal error probability provides upper and lower bounds on bit error probability, given by

$$\frac{1}{4} P_s(E) \leq P_b(E) \leq P_s(E) \quad (3.10)$$

However, an exact calculation of $P_b(E)$ is of considerable interest for comparing two modulation schemes. To do that we establish the following theorem.

Theorem:

In the presence of additive white Gaussian noise (AWGN) any modulation scheme which uses all the vertices of some hyper cube as signal space geometry, and an optimum receiver for detection has bit error probability given by

$$P_b(E) = Q\left(\sqrt{\frac{2E_b}{N_0}}\right) \quad (3.11)$$

where E_b is the average bit energy and $N_0/2$ is the two sided spectral density of AWGN. This probability of error holds for any dimension N of the hyper cube. The hyper cube is assumed to be placed symmetrically around the origin to minimize the requirement of average bit energy.

Proof:

Suppose the hyper cube is of dimension N . Then the number of signals in the modulated signal set is 2^N ; each of these signals represents a combination of N bits. If $P_{bi}(E)$ is the probability of error in the i^{th} bit position, then the average bit error probability is

$$P_b(E) = \frac{1}{N} \sum_{i=1}^N P_{bi}(E) = P_{b1}(E) \quad (3.12)$$

where the last equality comes from the equality of $P_{bi}(E)$ for all i because of the symmetry in signal space geometry. To calculate $P_{b1}(E)$ let us divide the signals into two sets: $\{(+1, a_2, a_3, \dots, a_N)\}$ and its image partner $\{(-1, a_2, a_3, \dots, a_N)\}$, where a_i 's

can be either of ± 1 with probability one half. These two sets of signals will lie on two parallel hyper planes of dimension $(N-1)$. Consider the midway hyper plane of the same dimension which separates the two sets and is equidistant from each original hyper plane. The distance of any signal in either set from the midway hyper plane is $d/2 = \sqrt{E_b/N} = \sqrt{E_b}$. Thus the signals with $+1$ in the first bit position are on one side of this plane at a distance $\sqrt{E_b}$ while the signals with -1 in the first bit position are on the other side at the same distance. So an error in the first bit position occurs only when the noise component $n(t)$ associated with this bit position drives a signal to the other side of the midway hyper plane. The probability of such an incident is

$$P_{b1}(E) = \int_{\sqrt{E_b}}^{\infty} p_n(x) dx = Q\left(\sqrt{\frac{2E_b}{N_0}}\right) \quad (3.13)$$

where $p_n(x)$ is the probability density function of Gaussian noise with variance per dimension of $N_0/2$. Hence the overall bit error probability is

$$P_b(E) = P_{b1}(E) = Q\left(\sqrt{\frac{2E_b}{N_0}}\right) \quad (3.14)$$

Since we have not assumed any particular value for N , probability of error given by (3.14) is valid for any dimension N of the hyper cube; hence the theorem is proved.

From equation (3.8) one may observe that for fixed p , as N becomes infinitely large, the signal error probability $P_s(E)$ goes to unity. On the other hand, the theorem asserts a bit error probability $P_b(E)$ independent of the dimension N . The explanation of this apparent contradiction lies in the following: the

theorem assumes a fixed bit energy E_b , so the signal energy E_s no longer remains fixed; it increases linearly with dimension N . Thus the distance between the two hyper planes containing $\{(+1, a_1, a_2, \dots, a_N)\}$ and $\{(-1, a_1, a_2, \dots, a_N)\}$ remains fixed at $d = 2\sqrt{E_b}$ and therefore $P_b(E)$ remains fixed while $P_s(E)$ does go to unity. The theorem illustrates that the hyper cube signal space geometry coupled with equiprobable use of all vertices is equivalent to antipodal binary geometry.

The bit error probability given by (3.14) implies that for a bit error rate of 10^{-5} , hyper cube signalling requires $E_b/N_0 = 9.12$ or 9.6 dB. BPSK uses two antipodal signals which can be considered as the vertices of a hyper cube of dimension one. Similarly QPSK and MSK, which use a set of four biorthogonal signals, can be considered as using the vertices of a hyper cube of dimension two. And Q^2PSK uses the vertices of a hyper cube of dimension four. So all of BPSK, QPSK, OQPSK, MSK and Q^2PSK belong to the same class of signalling schemes which use vertices of some hyper cube, and each of them has an energy efficiency 9.6 dB; this is true when the channel is wideband and corrupted only by AWGN.

If the channel is bandlimited, as it happens to be in many practical situations, each of the schemes responds differently. Due to intersymbol interference, signal space geometry no longer remains hyper cube and the energy efficiency is changed. To analyze the energy efficiency in bandlimited situations one needs to know about the power spectral distribution and the effect of bandlimiting on signal space geometry. Next we will discuss power spectral density and the effect of bandlimiting on bit error rate performance.

3.4 Spectral Density and Effect of Bandlimiting

Power Spectral Density

One can represent a Q^2PSK signal as

$$s_{q^2psk}(t) = \frac{1}{\sqrt{T}} a_1(t) p_1(t) \cos 2\pi f_c t + \frac{1}{\sqrt{T}} a_2(t) p_2(t) \cos 2\pi f_c t + \frac{1}{\sqrt{T}} a_3(t) p_1(t) \sin 2\pi f_c t + \frac{1}{\sqrt{T}} a_4(t) p_2(t) \sin 2\pi f_c t \quad (3.15)$$

where the additional $1/\sqrt{T}$ is just a normalizing factor to make $1/\sqrt{T} \cos\left(\frac{\pi t}{2T}\right)$ and $1/\sqrt{T} \sin\left(\frac{\pi t}{2T}\right)$ unit energy pulses. Data streams $a_i(t)$'s are assumed independent and at any instant each $a_i(t)$ can be either +1 or -1 with probability one half. So in each $2T$ second interval the Q^2PSK signal can be one of sixteen possible equally probable waveforms. Let us represent these waveforms by $m_i(t)$, i varying from 1 to 16. Probability of occurrence of $m_i(t)$ is $p_i = 1/16$ for all i . The signal set $\{m_i(t)\}$ has the following characteristics:

- (i) for each waveform $m_i(t)$, there is also a waveform $-m_i(t)$
- (ii) the probability of $m_i(t)$ and $-m_i(t)$ are equal
- (iii) the probability of transition between any two waveforms is the same.

Such a signalling source is said to be negative equally probable (NEP); the overall spectral density is given by [19]

$$S_{q^2psk}(f) = \sum_{i=1}^{16} p_i |M_i(f)|^2 \quad (3.16)$$

where $M_i(f)$ is the Fourier transform of $m_i(t)$ and is given by

$$M_i(f) = \int_{-\infty}^{\infty} m_i(t) e^{-j2\pi ft} dt.$$

One may reasonably assume the carrier frequency $f_c \gg \frac{1}{T}$; then for $f > 0$, each $M_i(f)$ is one of the following sixteen possible combinations.

$$\frac{1}{2} \left(\pm P_1(f-f_c) \pm P_2(f-f_c) \pm j P_1(f-f_c) \pm j P_2(f-f_c) \right)$$

where $P_1(f)$ and $P_2(f)$ are the Fourier transforms of the time-limited data shaping pulses (normalized without any change in the notation) $p_1(t)$ and $p_2(t)$ given by

$$p_1(t) = \frac{1}{\sqrt{T}} \cos \frac{\pi t}{2T} \quad |t| < T \quad (3.17)$$

$$p_2(t) = \frac{1}{\sqrt{T}} \sin \frac{\pi t}{2T} \quad |t| < T. \quad (3.18)$$

Substituting the $M_i(f)$'s into (3.16) and noticing that all cross terms cancelled, one may write

$$S_{q^2_{psk}}(f) = \frac{1}{2} \left[|P_1(f-f_c)|^2 + |P_2(f-f_c)|^2 \right], \quad f \geq 0. \quad (3.19)$$

The equivalent baseband version of the power spectral density is

$$S_{q^2_{psk}}(f) = \frac{1}{2} \left(|P_1(f)|^2 + |P_2(f)|^2 \right). \quad (3.20)$$

The Fourier transforms of the data shaping pulses are

$$P_1(f) = \frac{4\sqrt{T}}{\pi} \left(\frac{\cos 2\pi f T}{1-16f^2 T^2} \right) \quad (3.21)$$

$$P_2(f) = -\frac{j16\sqrt{T}}{\pi} \left(\frac{f T \cos 2\pi f T}{1-16f^2 T^2} \right). \quad (3.22)$$

Substituting (3.21) and (3.22) into (3.20), the baseband power spectral density

$S_{q^2_{psk}}(f)$ is given by

$$\frac{1}{T} S_{qpsk}(f) = \left(\frac{8}{\pi^2} \right) \left(1 + 16f^2 T^2 \right) \left(\frac{\cos 2\pi f T}{1 - 16f^2 T^2} \right)^2 \quad (3.23)$$

Similarly power spectral densities of *MSK* and *OQPSK* signalling schemes are given by

$$\frac{1}{T} S_{msk}(f) = \left(\frac{16}{\pi^2} \right) \left(\frac{\cos 2\pi f T}{1 - 16f^2 T^2} \right)^2 \quad (3.24)$$

$$\frac{1}{T} S_{oqpsk}(f) = 2 \left(\frac{\sin 2\pi f T}{2\pi f T} \right)^2 \quad (3.25)$$

where in all cases,

$$\int_{-\infty}^{\infty} S(f) df = 1$$

Power spectral densities of *OQPSK*, *MSK* and *Q²PSK* are sketched in Figure 3.3 as functions of normalized frequency f/R_b , where R_b , the bit rate, is $1/T$ for *MSK* and $2/T$ for *Q²PSK*. It should be noted that for a given bit rate, the width of the main lobe in *Q²PSK* is just half of the width of the *MSK* main lobe. *Q²PSK* uses two different kinds of data pulses; one is $p_1(t)$ having a cosinusoidal shape as in *MSK*, the other is $p_2(t)$ having a sinusoidal shape. The shape of $p_1(t)$ is smoother than $p_2(t)$ in the sense that the latter has jumps at $t = \pm T$; as a result, for large f , the spectral fall-off associated with $p_2(t)$ is proportional to f^{-2} while that with $p_1(t)$ is as f^{-4} . The faster fall-off associated with cosinusoidal shape causes lower side lobes in *MSK*; side lobes in *OQPSK* and *Q²PSK* are of the same order in magnitude but relatively higher than those of *MSK*. But a look into the spectral lobes does not give quantitative information about the spectral efficiencies; for that we need a measure of spectral compactness.

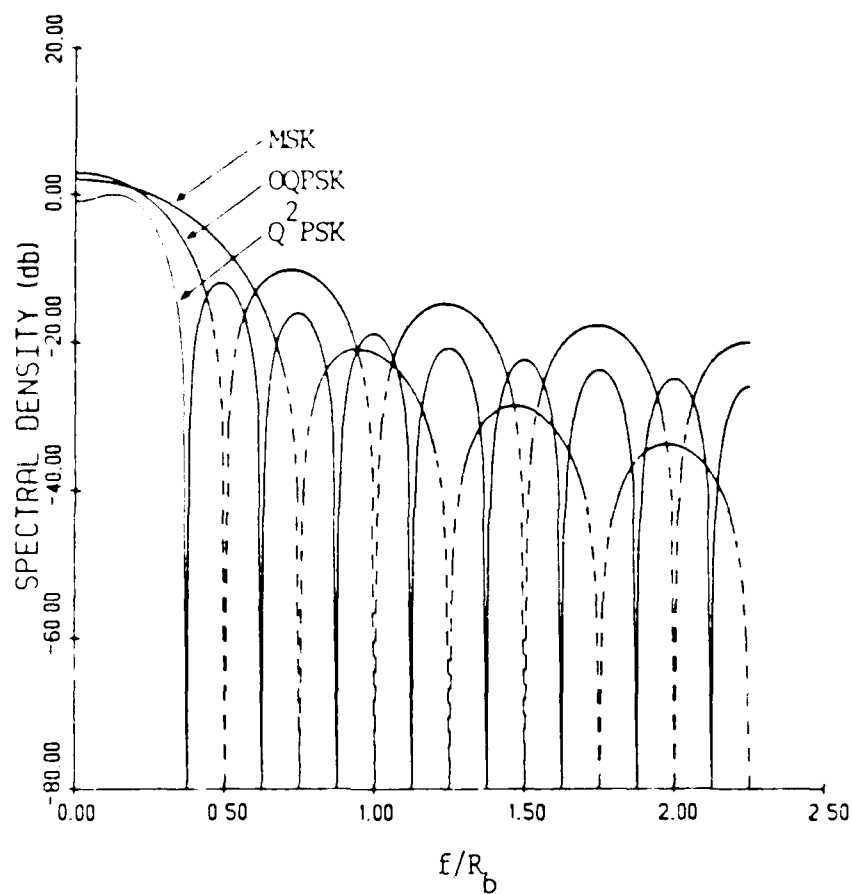


Figure 3.3. Spectral densities of OQPSK, MSK and Q^2PSK modulated signals.

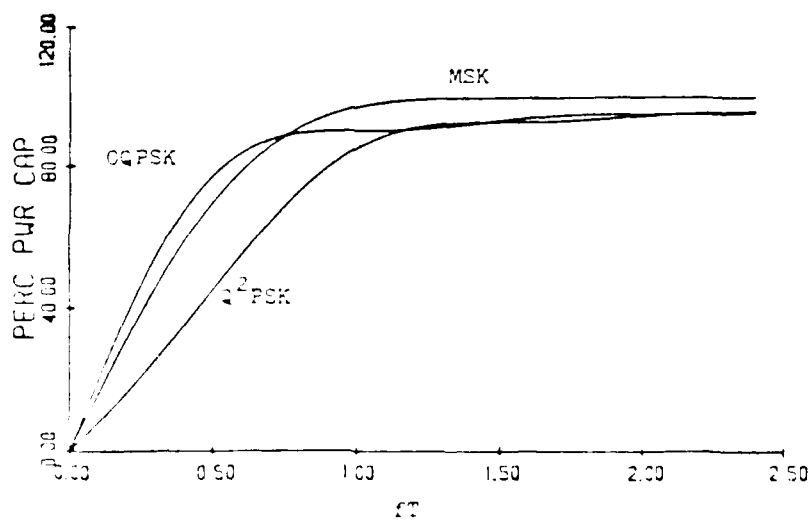


Figure 3.4. Percent power captured as function of bandwidth of MSK, OQPSK and Q^2PSK signals.

A measure of spectral compactness is the percent of total power captured in a specified bandwidth. This is plotted in Figure 3.4. For small bandwidth, the percent power captured in Q^2PSK is smaller than that in $OQPSK$ and MSK . Beyond a bandwidth of $1.2/T$, the asymptotic behavior of $QPSK$ and Q^2PSK become almost identical because of their same type of spectral fall-off as f^{-2} . MSK captures 99.1% of total spectral power in a bandwidth of $W = 1.2/T$. With $W = 1.2/T$, the power captured in $QPSK$ and Q^2PSK are 90.6 and 91.13 percent respectively. Thus MSK is more spectrally compact than Q^2PSK ; yet the bandwidth efficiency of Q^2PSK is higher because its data transmission rate is twice that of MSK . An exact calculation of bandwidth efficiency depends on the definition of bandwidth and the effect of bandlimiting on signal space geometries.

Effect of Bandlimiting

Consider an MSK scheme which allows a bandwidth of $\frac{1.2}{T}$ so that almost the entire spectrum (99.1% power) is available at the receiver. Suppose the MSK modulator is replaced by a Q^2PSK modulator and the modulator output is bandlimited by a multi-pole Butterworth filter with 3dB bandwidth equal to $1.2/T$ around the carrier frequency f_c . Our object is to compare the energy and the bandwidth efficiencies of the bandlimited Q^2PSK with the MSK scheme.

Thus, we assume the definition of channel bandwidth as $W = 1.2/T$. The bit rate in MSK then being $R_b^{MSK} = 1/T$, and the bandwidth efficiency is $b_{MSK} = 0.83$. The bit rate and the bandwidth efficiency of Q^2PSK are $R_b^{Q^2PSK} = 2/T$ and

$b_{q^2psk} = 1.66$ respectively. Thus there is a one hundred percent increase in the bandwidth efficiency over *MSK* without any change in bandwidth; this increase is evidently due to increase in the dimensionality of the signal space.

With the above definition of channel bandwidth, an *MSK* signal gets through almost undistorted; so the energy efficiency is maintained at its ideal value of 9.6 dB. A *Q²PSK* scheme, on the other hand, when bandlimited to $1.2/T$, allows transmission of only 91.13% of total spectral power. Thus there is a loss of some spectral components: this loss causes spread of the baseband data pulses which in turn causes intersymbol interference (ISI). After bandlimiting, the baseband signal associated with either carrier is of the following form

$$s_{q^2psk}^b(t) = \frac{A}{\sqrt{T}} \sum_{k=-\infty}^{\infty} \left(a_{1,k} p_{1b}(t-2kT) + a_{2,k} p_{2b}(t-2kT) \right), \quad (3.26)$$

where A is an amplitude factor, $p_{1b}(t)$ and $p_{2b}(t)$ are the bandlimited versions of data pulses $p_1(t)$ and $p_2(t)$, and $a_{i,k}$'s being either $+1$ or -1 represent the information bits over the interval $(k-1)T < t < (k+1)T$.

Squaring both sides of (3.26) one can write the squared bandlimited signal as

$$\begin{aligned} \left(s_{q^2psk}^b(t) \right)^2 &= \frac{A^2}{T} \left[\sum_k \left\{ p_{1b}^2(t-2kT) + p_{2b}^2(t-2kT) \right\} + \right. \\ &\quad 2 \sum_j \sum_{k(j \neq k)} a_{1,j} a_{1,k} p_{1b}(t-2jT) p_{1b}(t-2kT) + \\ &\quad 2 \sum_j \sum_{k(j \neq k)} a_{2,j} a_{2,k} p_{2b}(t-2jT) p_{2b}(t-2kT) + \\ &\quad \left. 2 \sum_j \sum_k a_{1,j} a_{2,k} p_{1b}(t-2jT) p_{2b}(t-2kT) \right]. \quad (3.27) \end{aligned}$$

The expected value of the squared signal is given by

$$E\left(s_{q,prk}^b(t)\right)^2 = \frac{A^2}{T} \left(\sum_k p_{1b}^2(t-2kT) + \sum_k p_{2b}^2(t-2kT) \right) \quad (3.28)$$

where we used the i.i.d. nature of data,

$$E \left(a_{1,j} a_{1,k} \right) = \delta_{j,k} \quad (3.29a)$$

$$E \left(a_{2,j} a_{2,k} \right) = \delta_{j,k} \quad (3.29b)$$

$$E \left(a_{1,j} a_{2,k} \right) = 0 \quad (3.29c)$$

where δ_{jk} is the Kronecker delta. Hence the average energy per transmission of each bit is given by

$$\begin{aligned} E_b &= \frac{1}{2} \int_{-T}^T E \left(s_{q,prk}^b(t) \right)^2 dt \\ &= \frac{1}{2} \frac{A^2}{T} \int_{-\infty}^{\infty} \left(p_{1b}^2(t) + p_{2b}^2(t) \right) dt \end{aligned} \quad (3.30)$$

In general, the bandlimited pulses $p_{1b}(t)$ and $p_{2b}(t)$ spread over several signalling intervals. If they spread over N_1 and N_2 signalling intervals respectively then for every information bit, the received signal level at the receiver can be one of the $2^{(N_1+N_2)}$ possible values. In order to get the average bit error probability, one needs to calculate the error probability for each of these situations. The number of computations and hence the computing time increases exponentially with (N_1+N_2) . A typical situation may require considering N_1 and N_2 of the order of twenty to get an accurate result. A dedicated IBM PC may require a week to do such computations. An alternative and convenient way of calculating the average bit error probability lies in finding the probability density function (pdf) of the received signal levels in the presence of noise; in this approach computing

time increases linearly with $(N_1 + N_2)$. This pdf approach is discussed in Appendix A. In the following and also in all future discussions we always follow this approach for calculating the bit error probability.

We considered several Butterworth filters of different orders and of different bandwidths for bandlimiting the ideal Q^2PSK modulated signal and evaluated the effect of bandlimiting on energy efficiency. The bit error rate performance of Q^2PSK alongwith those of MSK and QPSK are shown in Figure 3.5; this performance evaluation assumed a sixth order Butterworth filter with 3dB bandwidth equal to $1.2/T$. For a bit error rate $P_b(E) = 10^{-6}$, Q^2PSK and MSK need 11.2 dB and 9.6 dB E_b/N_0 respectively. Thus Q^2PSK achieves twice the bandwidth efficiency of MSK at the expense of 1.6 dB increase in the average bit energy.

To achieve twice the bandwidth efficiency of MSK, Q^2PSK thus pays forty five percent increase in the average bit energy. One may like to compare this increase with the increase in bit energy required by a multilevel MSK having the same bandwidth efficiency as the bandlimited Q^2PSK . The set of four signals used in ordinary MSK is biorthogonal; the data pulse associated with each of the two carriers is either a positive or a negative cosine pulse of duration $2T$, i.e. the possible numbers of levels in the basic data pulse is two. For a multilevel MSK, in order to achieve twice the bandwidth efficiency of biorthogonal MSK, the number of amplitude levels in the data pulse must be four. For such a four level MSK, the bit error probability [Appendix B] is given by

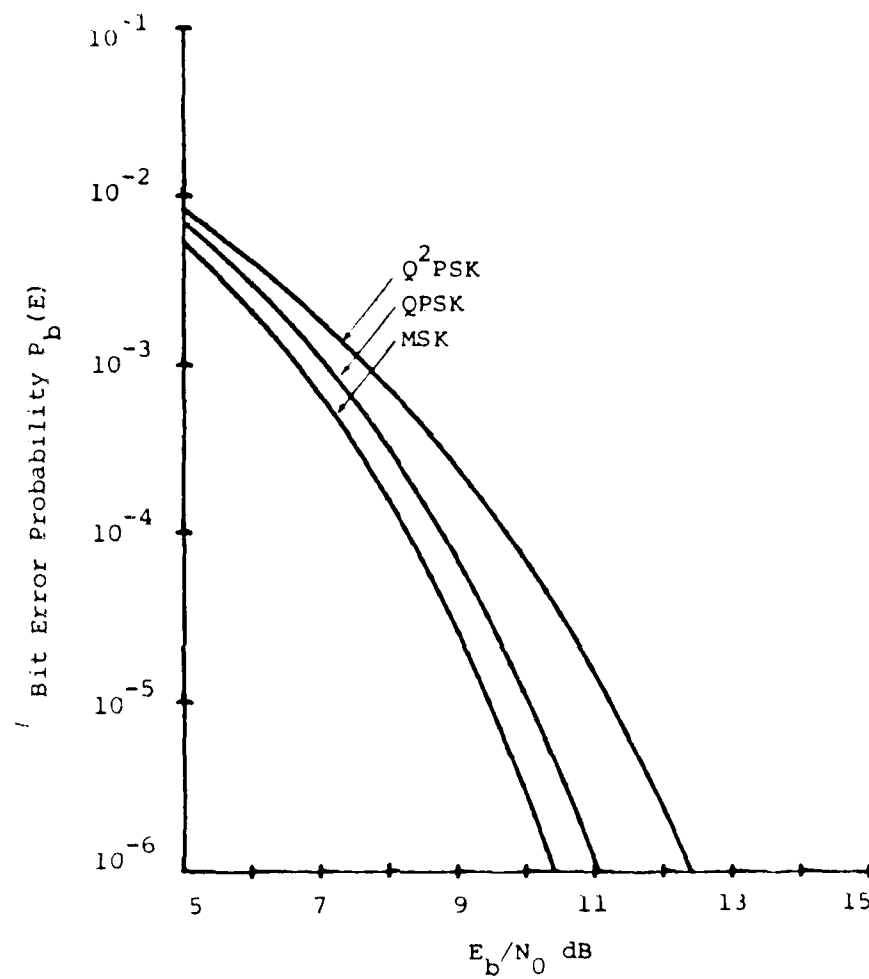


Figure 3.5. Bit error probabilities as functions of E_b/N_0 for Q^2PSK , QPSK and MSK signals.

$$P_b(E) = \frac{1}{4} \left\{ 3 Q(r) + 2 Q(3r) - Q(5r) \right\} \quad (3.31)$$

where,

$$r = \sqrt{\frac{4E_b}{5N_0}} \quad (3.32)$$

and the function $Q(\cdot)$ is defined in (3.9b). It follows from (3.31) that for a bit error rate of 10^{-5} , a four-level MSK requires 13.4 dB E_b/N_0 . Thus in achieving twice bandwidth efficiency of biorthogonal MSK, the four-level MSK requires about 142% increase in the average bit energy; whereas with Q^2PSK the increment is 45% only. Thus Q^2PSK turns out to be a more energy efficient candidate to increase the bandwidth efficiency by a factor of two over ordinary or biorthogonal MSK. Results of this section are summarized in the following table.

TABLE 3.1
Energy and Bandwidth Efficiencies
of Q^2PSK , two and four-level MSK
 $W = 1.2/T$

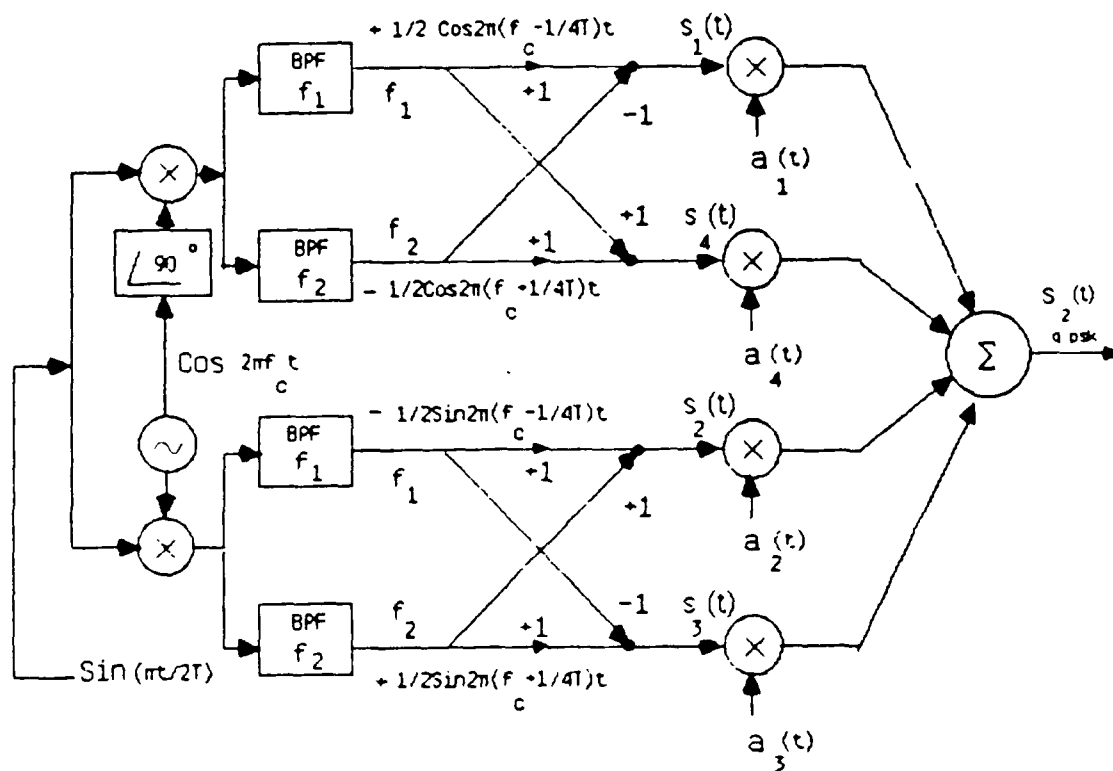
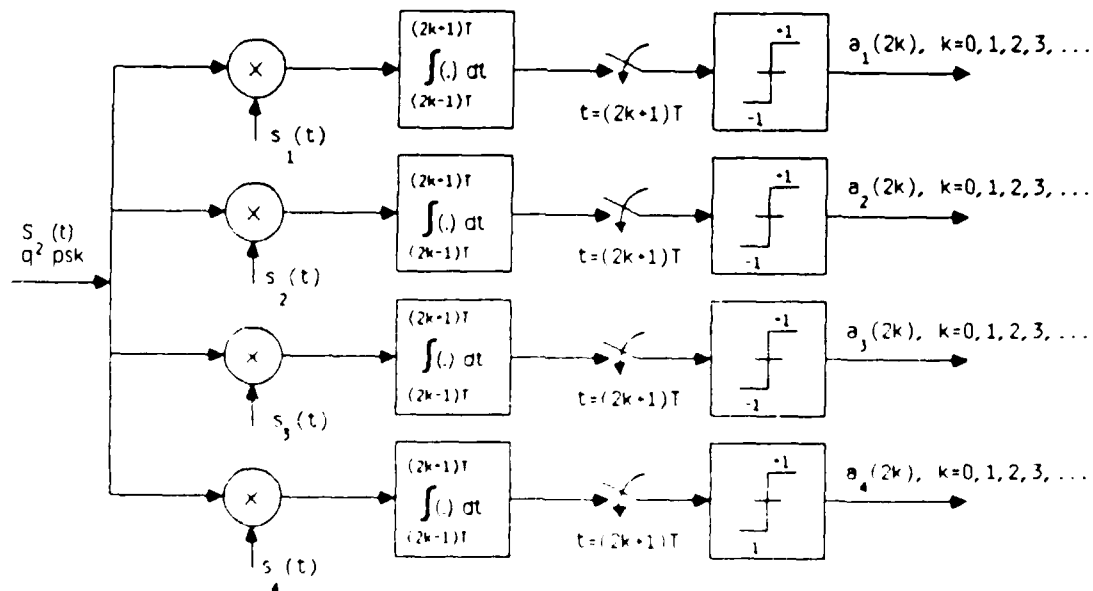
Type of modulation	MSK biorthogonal	Q^2PSK	MSK Four-level
Bandwidth efficiency	0.83	1.66	1.66
E_b/N_0 for $P_b(E) = 10^{-5}$	9.8 dB	11.2 dB	13.4 dB

3.5 Modulator Demodulator and Synchronization Scheme

A block diagram of a Q^2PSK modulator is shown in Figure 3.6. Two phase coherent sine and cosine carriers are multiplied by an external clock signal at one eighth the bit rate to produce phase coherent sine and cosine signals of frequencies $f_1 = f_c - \frac{1}{4T}$ and $f_2 = f_c + \frac{1}{4T}$. These signals are then separated by means of narrow bandpass filters and combined with appropriate polarity to form the basis signal set $\left\{ s_i(t) \right\}_{i=1}^4$ of equation (3.1). The advantage of deriving the basis signals in this fashion (instead of generating them independently) is that the signal coherence and the deviation ratio are largely unaffected by any small variation in the incoming data rate [20]. These basis signals are multiplied by the demultiplexed data streams and then added to form the $Q^2 PSK$ signal defined in (3.4).

A block diagram of the Q^2PSK demodulator is shown in Figure 3.7. The received signal is multiplied by each of the basis signals individually and integrated over an interval of $2T$. This multiplier integrator combination constitutes correlation detection or matched filtering, an optimum coherent receiver in the absence of ISI. Binary decisions followed by integrators give an estimate of the four binary data streams $a_i(t)$, $i=1,2,3,4$.

One of the basic problems in coherent demodulation is the recovery of the modulating signal phase and bit timing information from the received signal. In an MSK receiver these two are derived from the received signal. In other words,

Figure 3.6. Realization of Q^2PSK - modulator.Figure 3.7. Realization of Q^2PSK - demodulator.

an MSK signal has self clocking and self synchronizing ability [20,21,22]. In the present situation, we need to recover the basis signal set $\{s_i(t)\}$ and a clock signal at one fourth the bit rate. These signals can be derived from the Q^2PSK modulated signal by a nonlinear operation, such as squaring, and appropriate filtering as shown in Figure 3.8.

If the $Q^2 PSK$ modulated signal (3.4) passes through a squaring device, at the output we get,

$$\begin{aligned}
 s_{Q^2PSK}^2(t) = & 1 + \frac{1}{2} \left(a_1 a_2 + a_3 a_4 \right) \sin \left(\frac{\pi t}{T} \right) \\
 & + \frac{1}{2} \left(a_1 a_2 - a_3 a_4 \right) \sin \left(\frac{\pi t}{T} \right) \cos(4\pi f_c t) \\
 & + \cos(\theta_{12} - \theta_{34}) \sin(4\pi f_c t) \\
 & + \cos(\theta_{12} + \theta_{34}) \cos \left(\frac{\pi t}{T} \right) \sin(4\pi f_c t) \\
 & + \sin(\theta_{12} + \theta_{34}) \sin \left(\frac{\pi t}{T} \right) \sin(4\pi f_c t)
 \end{aligned} \tag{3.33}$$

where,

$$\theta_{12}(t) = \tan^{-1} \left(\frac{a_2(t)}{a_1(t)} \right) \tag{3.34a}$$

and

$$\theta_{34}(t) = \tan^{-1} \left(\frac{a_4(t)}{a_3(t)} \right). \tag{3.34b}$$

There are five components on the right of (3.33) which carry the required clocking and carrier phase information. The expected value of each of these five

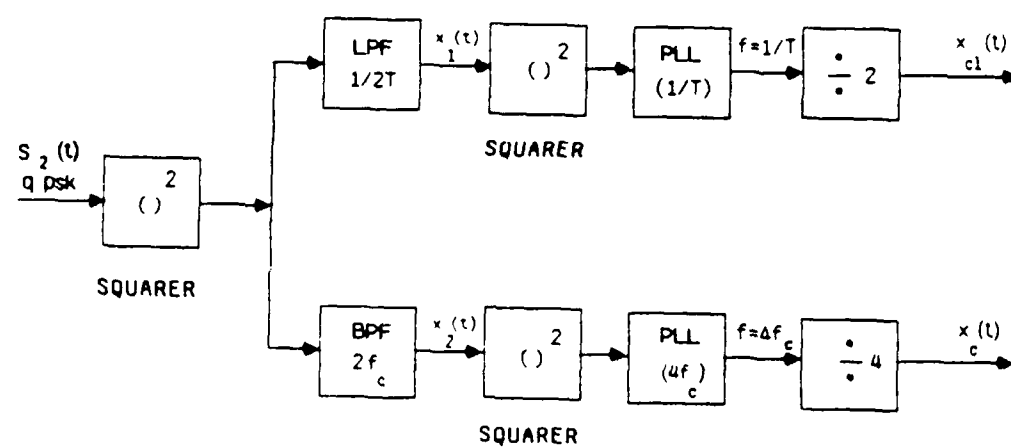


Figure 3.8. Synchronization scheme for coherent demodulation of Q^2PSK signal.

components is zero. So to recover the clocking and the carrier phase information, we need filtering and further nonlinear operation. By a lowpass and a bandpass filtering of the squared signal, one may construct two signals $x_1(t)$ and $x_2(t)$ as

$$x_1(t) = \frac{1}{2} (a_1 a_2 + a_3 a_4) \sin \left(\frac{\pi t}{T} \right) \quad (3.35)$$

$$x_2(t) = \cos(\theta_{12} - \theta_{34}) \sin(4\pi f_c t). \quad (3.36)$$

After squaring $x_1(t)$, $x_2(t)$ and taking the expectation

$$E \left(x_1^2(t) \right) = \frac{1}{4} \left(1 - \cos \frac{2\pi t}{T} \right), \quad (3.37)$$

$$E \left(x_2^2(t) \right) = \frac{1}{4} \left(1 - \cos 8\pi f_c t \right). \quad (3.38)$$

Thus, on the average, $x_1^2(t)$ and $x_2^2(t)$ contain spectral lines at $\frac{1}{T}$ and $4f_c$.

One can use these lines to lock phase-locked loops and carry out frequency divisions to recover the clocking and the carrier information as

$$x_{cl}(t) = \cos \frac{\pi t}{T} \quad (3.39)$$

and

$$x_c(t) = \cos 2\pi f_c t \quad (3.40)$$

Signal $x_{cl}(t)$ provides timing information at a rate of one fourth the bit rate; this timing information is essential for sampling the integrator output in the demodulator (Figure 3.7). The basis signal set $\{ s_i(t) \}$ required in the process of demodulation can be constructed easily by simple manipulation of the signals $x_{cl}(t)$ and $x_c(t)$. Recovery of $x_{cl}(t)$ and $x_c(t)$ from the received signal $s_{q, \text{peak}}(t)$ has been illustrated in block diagram in Figure 3.8.

3.6 Summary

Quadrature-Quadrature phase shift keying is a new kind of spectrally efficient modulation scheme which makes effective use of available signal space dimensions by the use of two orthogonal data shaping pulses on each of the two orthogonal carriers. It increases the bandwidth efficiency by a factor of two over MSK at the expense of 1.6 dB increase in the average bit energy. It can also be viewed as two minimum shift keying type signalling schemes in parallel. Compact power spectrum, good error rate performance, and self-synchronizing ability make Q^2PSK an attractive digital modulation scheme.

CHAPTER FOUR

QUADRATURE-QUADRATURE PHASE SHIFT KEYING : A CONSTANT ENVELOPE MODULATION SCHEME

4.1 Introduction

In designing a modulation scheme, though energy and bandwidth efficiencies are two important criterion, constant envelope may be an additional desirable feature for certain nonlinear type of channels. For instance, the travelling wave tube (TWT) amplifier in a satellite repeater usually converts amplitude variations to spurious phase modulation. A constant envelope in the modulated signal may reduce this problem to a great extent [3,10,23]. Also if there is some non-linearity in the channel due to the presence of class C devices, constant envelope may be an additional desirable feature. This envelope property of MSK is one of the main attributes which makes MSK so popular for both linear and nonlinear channels. It is observed that without any additional constraint, the Q^2PSK signal does not maintain a constant envelope. However, it has been found that a simple block coding prior to the modulation permits a constant envelope in the modulated signal. Next we will discuss the coding scheme and analyze the energy and the bandwidth efficiencies of the coded Q^2PSK signal. The coding action alters some spectral properties of the signal; as a result the synchronization scheme

given in the last chapter will not work for the coded scheme. A different synchronization scheme is presented for the coherent demodulation of the coded signal.

4.2 Constant Envelope Q²PSK

One can write the Q²PSK signal (3.4) as

$$s_{q^2psk}(t) = A(t) \cos(2\pi f_c t + \theta(t)) \quad (4.1)$$

where $\theta(t)$ is the carrier phase and $A(t)$ is the carrier amplitude given by,

$$A(t) = \left(2 + (a_1 a_2 + a_3 a_4) \sin \frac{\pi t}{T} \right)^{1/2}. \quad (4.2)$$

Without any additional constraint the envelope of the Q²PSK signal is not constant; it varies with time. In order to maintain a constant envelope let us consider a simple block coding at the input of the Q²PSK modulator : the coder accepts serial input data and for every three information bits $\{ a_1, a_2, a_3 \}$, it generates a codeword $\{ a_1, a_2, a_3, a_4 \}$ such that the first three bits in the code word are the information bits and the fourth one is an odd parity check for the information bits. The rate of the code is 3/4. One can write the parity check bit $a_4(t)$ as

$$a_4(t) = \frac{a_1(t)a_2(t)}{a_3(t)} \quad (4.3)$$

Substituting (4.3) into (4.2) one may observe that if this coded bit stream is modulated using Q^2PSK format, a constant envelope is maintained [15]. This additional envelope feature is achieved at the sacrifice of bandwidth efficiency; the information transmission rate is reduced from $R_b=2/T$ to $R_b=3/2T$.

Four of the eight possible code words $\{C_i\}_{i=1}^8$ are follows:

$$C_1=(+ + + -)$$

$$C_2=(+ + - +)$$

$$C_3=(+ - + +)$$

$$C_4=(+ - - -)$$

The remaining four code words are just the negatives of these. This is a set of eight biorthogonal codes with a minimum Hamming distance $d_{\min}=2$. In analyzing the performance of this coded scheme, hard decisions are assumed at the receiver. The code therefore cannot be used for error correction. The redundant information associated with the fourth demultiplexed data stream $a_4(t)$ can, however, be used to improve the signal to noise performance of the code.

In a practical situation when the signal is bandlimited, the biorthogonal structure of the code is destroyed due to intersymbol interference. In Q^2PSK format there are two data shaping pulses: one is a smooth half cosinusoid associated with data streams $a_1(t)$ and $a_3(t)$; the other is a half sinusoid associated with $a_2(t)$ and $a_4(t)$. On bandlimiting, the half sinusoid, because of its sharp discontinuities at the ends, gets relatively more distorted than the half cosinusoid. So

we assume that, at the receiver, the redundant information associated with $a_4(t)$ is used only in making the binary decision about the information bits in $a_2(t)$; the decision about the information bits in $a_1(t)$ and $a_3(t)$ are made independently from the observations on the respective pulse trains only. A block diagram of the demodulator is shown in Figure 4.1.

To make a decision about a_2 , we make a simplifying assumption that a_1 and a_3 are decoded correctly. Correctly made decisions of a_1 and a_3 along with the estimates a_{2r} of a_2 and its redundant version a_{4r} of a_4 are then the observations for making decision about a_2 . It can be shown that a sufficient statistic for making this decision is the random variable V given by [Appendix C],

$$V = a_{2r} - \frac{a_1}{a_3} a_{4r} . \quad (4.4)$$

A decoder, which is optimum in the sense of minimizing the probability of error, will take a decision a_2 as +1 or -1 according as $V \geq 0$ or $V < 0$. However, formation of the right decision statistic (V) is subject to the correctness of the decision about a_1 and a_3 . Let p_1 and p_3 be the probability of error in making decisions about a_1 and a_3 , and q be the probability of error in decision of a_2 when decision is based on the correct decision statistic (V). Then the actual probability of error in a_2 is given by

$$p_2 = q + p_1(1-p_1)(1-2q) . \quad (4.5)$$

In evaluating the performance of the scheme, bandlimiting has been allowed at both receiver and transmitter through the use of sixth order Butterworth filters with half power bandwidth equal to $1.2/T = 0.83 R_b$. It has been found

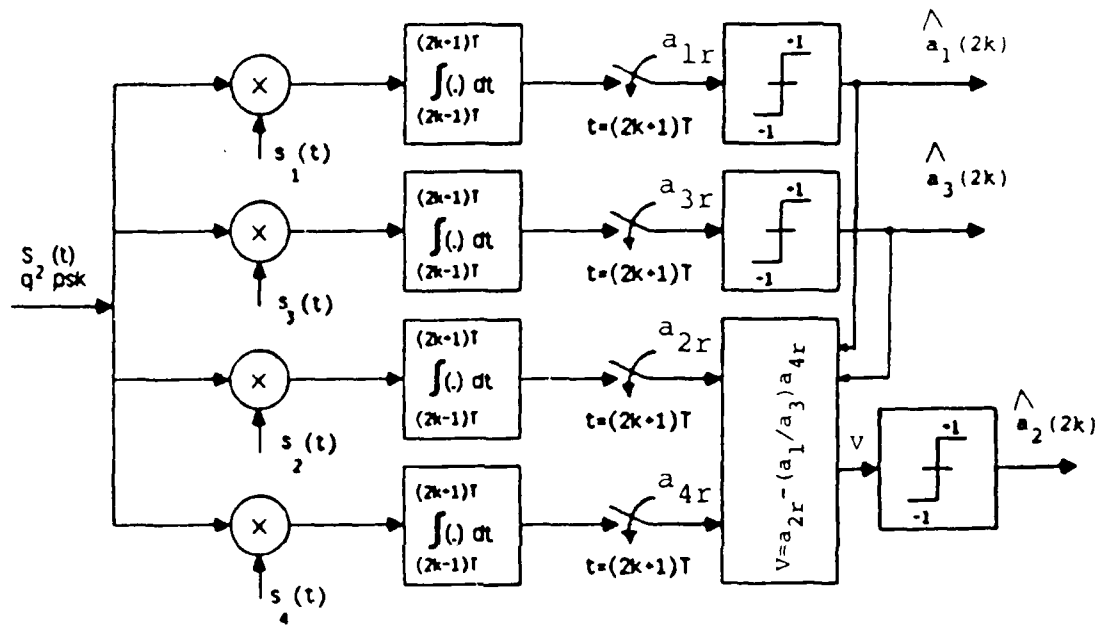


Figure 4.1. Constant envelope Q^2PSK - demodulator.

that for a bit error rate of 10^{-5} , the constant envelope scheme requires an $E_b/N_0 = 10.3$ dB while for MSK $E_b/N_0 = 9.6$ dB. Thus there is 50% increase in the bandwidth efficiency over MSK at the cost of 0.7 dB increase in the average bit energy; both schemes have constant envelopes. Bit error probability of the coded Q^2PSK alongwith those of MSK and TFM have been plotted against E_b/N_0 in Figure 4.2.

The above evaluation of performance is based on the assumption of bit by bit detection. With symbol by symbol detection, one may utilize the Euclidean distances among the signal points of coded Q^2PSK (which are biorthogonal) more efficiently and make considerable improvement in energy efficiency. The bit error rate performance based on symbol by symbol detection in the absence of bandlimiting [24] has also been shown in Figure 4.2. In the absence of bandlimiting, with symbol by symbol detection (i.e. optimum detection) the E_b/N_0 requirement of coded Q^2PSK for a bit error rate of 10^{-5} is about 7.4 dB. The performance in the bandlimited situation has not been studied.

4.3 Demodulation and Synchronization

A block diagram of the receiver which performs coherent demodulation of the coded Q^2PSK signal is shown in Figure 4.1. To implement this matched filter receiver one needs to know carrier phase and bit timing information. Because of the effect of coding the synchronization scheme we discussed in the previous chapter will not work in the present situation [15]. A different but a similar synchronization scheme has been presented in Figure 4.3.

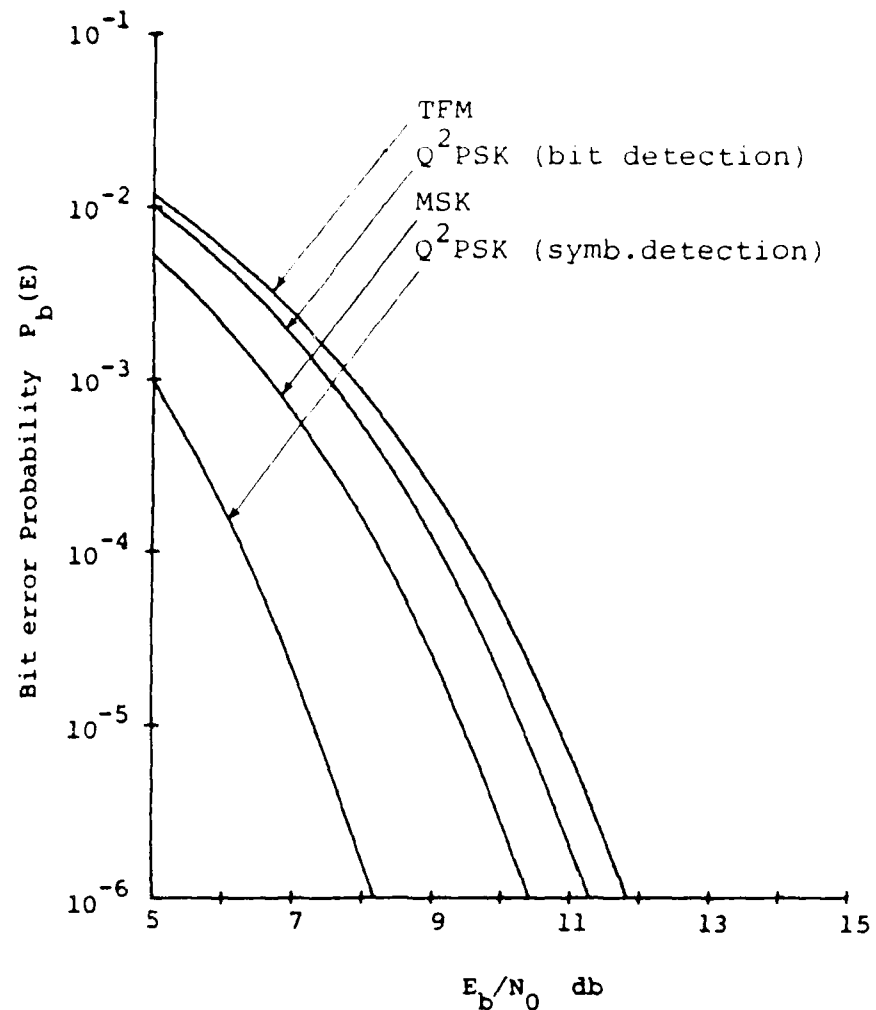


Figure 4.2. Bit error probabilities as functions of E_b/N_0 for MSK, TFM and coded Q^2PSK .

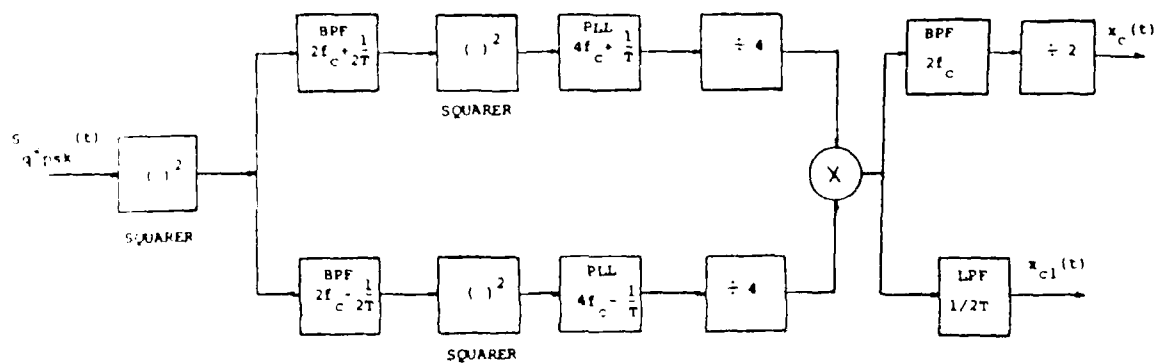


Figure 4.3. Synchronization scheme for coherent demodulation of constant envelope Q^2PSK signal.

If the Q^2 PSK modulated signal defined by (3.4) passes through a squaring device, at the output we get,

$$\begin{aligned}
 s_{q^2psk}^2(t) = & 1 + \frac{1}{2} (a_1 a_2 + a_3 a_4) \sin \left(\frac{\pi t}{T} \right) \\
 & + \frac{1}{2} (a_1 a_2 - a_3 a_4) \sin \left(\frac{\pi t}{T} \right) \cos(4\pi f_c t) \\
 & + \cos(\theta_{12} - \theta_{34}) \sin(4\pi f_c t) \\
 & + \cos(\theta_{12} + \theta_{34}) \cos \left(\frac{\pi t}{T} \right) \sin(4\pi f_c t) \\
 & + \sin(\theta_{12} + \theta_{34}) \sin \left(\frac{\pi t}{T} \right) \sin(4\pi f_c t)
 \end{aligned} \tag{4.6}$$

where,

$$\theta_{12}(t) = \tan^{-1} \left(\frac{a_2(t)}{a_1(t)} \right) \text{ and} \tag{4.7a}$$

$$\theta_{34}(t) = \tan^{-1} \left(\frac{a_4(t)}{a_3(t)} \right). \tag{4.7b}$$

Substituting the parity check condition $a_4 = -a_1 a_2 / a_3$, one can simplify (4.6) as

$$\begin{aligned}
 s_{q^2psk}^2(t) = & 1 + \frac{1}{2} (a_1 a_3 + a_1 a_2) \sin \left[2\pi t (2f_c + \frac{1}{2T}) \right] \\
 & + \frac{1}{2} (a_1 a_3 - a_1 a_2) \sin \left[2\pi t (2f_c - \frac{1}{2T}) \right]
 \end{aligned} \tag{4.8}$$

There are two components on the right of (4.8) which carry the required clocking and carrier phase information. The expected value of each of these two components is zero. So the recovery of the clocking and the carrier phase informa-

tion requires filtering and further nonlinear operation. By bandpass filtering of the squared signal one may construct two signals $x_1(t)$ and $x_2(t)$ as

$$x_1(t) = \frac{1}{2} (a_1 a_3 + a_1 a_2) \sin \left(2\pi t \left(2f_c + \frac{1}{2T} \right) \right) \quad (4.9)$$

$$x_2(t) = \frac{1}{2} (a_1 a_3 - a_1 a_2) \sin \left(2\pi t \left(2f_c - \frac{1}{2T} \right) \right). \quad (4.10)$$

After squaring $x_1(t)$, $x_2(t)$ and taking the expectation one can show

$$E(x_1^2(t)) = \frac{1}{4} \left(1 - \cos 2\pi t \left(4f_c + \frac{1}{T} \right) \right) \quad (4.11)$$

and

$$E(x_2^2(t)) = \frac{1}{4} \left(1 - \cos 2\pi t \left(4f_c - \frac{1}{T} \right) \right). \quad (4.12)$$

Thus $x_1^2(t)$ and $x_2^2(t)$ contains spectral lines at $4f_c \pm \frac{1}{T}$. One can use these lines to lock phase-locked loops, and carry out frequency divisions so as to form the signals $x_3(t)$ and $x_4(t)$ as

$$x_3(t) = \cos 2\pi t \left(f_c + \frac{1}{4T} \right) \quad (4.13)$$

$$x_4(t) = \cos 2\pi t \left(f_c - \frac{1}{4T} \right). \quad (4.14)$$

A multiplication of these two signals followed by bandpass filtering and frequency division gives clocking and carrier phase information as

$$x_{cl}(t) = \cos \frac{\pi t}{T} \quad (4.15)$$

and

$$x_c(t) = \cos 2\pi f_c t . \quad (4.16)$$

Signal $x_d(t)$ provides timing information at a rate of $1/2T$; this timing information is essential for sampling the integrator output in the demodulator (see Figure 4.1). A block diagram of the synchronization scheme is shown in Figure 4.3. The basis signal set $\{ s_i(t) \}$ required in the process of demodulation can be constructed easily by simple manipulation of the signals $x_d(t)$ and $x_c(t)$.

4.4 Summary

Quadrature-Quadrature Phase Shift Keying has twice the bandwidth efficiency of MSK; but unlike MSK, it does not have a constant envelope. A simple parity check coding, however, creates a constant envelope signal. The bandwidth efficiency of this coded Q^2PSK is 1.5 times that of MSK. With a receiver based on the assumption of bit by bit detection and for a bit error rate of 10^{-6} the average bit energy requirement of this scheme is about 0.8 dB higher as compared to MSK. However, with symbol by symbol detection the bit energy requirement is expected to be much lower than that of MSK. The scheme possesses self clocking and self synchronizing ability.

CHAPTER FIVE

GENERALIZED

QUADRATURE-QUADRATURE PHASE SHIFT KEYING

5.1 Introduction

The original Q^2PSK uses two data shaping pulses and two carriers to form a four dimensional signal space. The idea can be generalized by incorporating n orthogonal data shaping pulses alongwith two orthogonal carriers to create a $2n$ -dimensional signal space. The original case of $n=2$ increased the bandwidth efficiency by a factor of two over MSK at the expence of 1.6 dB increase in the average bit energy. The requirement of higher bit energy is due to bandlimiting effect on one of the two pulses used for data shaping. In an attempt to generalize the scheme in higher dimension, attention has been paid to the smoothness of the data shaping pulses so that spectral density falls off faster than that of original Q^2PSK . For example, the extra bit energy requirement can be avoided by allowing $n > 0.5$ in the bandwidth efficiency; in a special case of $n = 3$ it will be shown that a bandwidth efficiency which is 1.6 times that of MSK is achieved without any increase in the average bit energy. This bandwidth efficiency is also 1.5

times that of QORC, which is a non constant envelope scheme but more spectrally compact than MSK.

5.2 Formulation of Generalized Q²PSK

Let $\left\{p_i(t)\right\}_{i=1}^n$ be a set of n data shaping components, which, along with two orthogonal carriers of frequency f_c , are used to modulate $2n$ i.i.d. binary data streams $\left\{a_i(t)\right\}_{i=1}^n$ and $\left\{b_i(t)\right\}_{i=1}^n$ such that the modulated signal is given by ,

$$s(t) = \sum_{i=1}^n a_i(t)p_i(t)\cos 2\pi f_c t + \sum_{i=1}^n b_i(t)p_i(t)\sin 2\pi f_c t \quad (5.1)$$

where,

$$\int_{(2k-1)T/2}^{(2k+1)T/2} p_i(t)p_j(t)dt = \delta_{ij} . \quad (5.2)$$

Each binary datum (± 1) in $a_i(t)$ and $b_i(t)$ is of duration T ; e.g. the k^{th} datum in any of the $2n$ streams appears over $(2k-1)T/2$ to $(2k+1)T/2$. The modulated signal space will be the vertices of a hypercube of dimension $2n$. The overall bit rate of the system is $R_b = 2n/T$. Signal $s(t)$ represents a generalized Q²PSK signal. The special case of $n=1$ is a two dimensional scheme such as QPSK, MSK or QORC. In chapter three we considered the special case of $n=2$ which is the original Q²PSK.

Phase and Spectral Properties of Q²PSK (n=2)

One can write Q²PSK (n=2) signal (3.4) as

$$s_{q^2psk}(t) = A(t) \cos(2\pi f_c t + \theta(t)) \quad (5.3)$$

where,

$$A(t) = \left(2 + (a_1 a_2 + a_3 a_4) \sin \frac{2\pi t}{T} \right)^{1/2} \quad (5.4a)$$

and

$$\theta(t) = \tan^{-1} \left(\frac{a_3 \cos \frac{\pi t}{T} + a_4 \sin \frac{\pi t}{T}}{a_1 \cos \frac{\pi t}{T} + a_2 \sin \frac{\pi t}{T}} \right). \quad (5.4b)$$

Symbol transitions occur at the instants $t = (2k+1)T/2$, where k is an integer; at those instants carrier phase $\theta(t)$ can be any one of the four possible values $\pm 45^\circ, \pm 135^\circ$. Thus an abrupt $\pm 90^\circ$ or 180° phase change in the RF carrier may occur at a symbol transition instant; the carrier does not maintain continuity in phase. In designing a modulation scheme, though energy and bandwidth efficiencies are two important criterion, continuity of phase in the RF signal may be an additional desirable feature in certain situations. With continuity in phase, high frequency content and therefore secondary sidelobes can be expected to be relatively lower in strength; in other words, spectrum fall-off will be sharper and so restrictions on the subsequent bandlimiting filter shapes can be relaxed. This is desirable in certain situations where filtering after modulation is cost prohibited and out of band radiation needs to be at a low level. Also in a bandlimited situation, faster spectral fall-off of the signal itself may result in less ISI and

hence less average bit energy requirement for a specified bit error rate. So it is quite reasonable to look for possibilities of continuity of phase in the Q^2PSK signal. In the literature one may find a wide variety of continuous phase modulations. Many of them use some sort of correlative coding which introduces finite memory into the modulated signal. In the following discussions we assume a zero memory modulation; in other words we do not use any correlative coding scheme in an attempt to obtain phase continuity in the signal.

The original Q^2PSK uses two data shaping pulses; one of them is a half sinusoid $p_2(t)$ defined in (3.2b). If one replaces the half sinusoid by a full sinusoid over the same signalling interval $|t| \leq T$, the RF carrier will have continuity in phase. The baseband spectral density of the Q^2PSK signal in this situation is given by

$$\frac{1}{T} S_{q^2psk}(f) = \frac{8}{\pi^2} \left(\frac{\cos 2\pi f T}{1-16f^2 T^2} \right)^2 + \frac{2}{\pi^2} \left(\frac{\sin 2\pi f T}{1-4f^2 T^2} \right)^2.$$

In spite of sharper asymptotic spectrum fall off, this version of Q^2PSK signal, for a finite transmission bandwidth, captures almost the same power as the original one. With 99% power bandwidth ($1.2/T$) of MSK as the transmission bandwidth, this new version captures only 89.9% of the radiated power while the original one captures 91.1%. The 99% power bandwidth of this new version is $1.75/T$. The new version, therefore, does not seem to be any better than the original one in energy efficiency unless a substantial loss in the bandwidth efficiency is suffered. With 99% power bandwidth of MSK as the transmission bandwidth, it requires 12.0 dB E_b/N_0 , which is 0.8 dB higher than the original one of 11.2 dB.

5.3 Q^2PSK ($n=3$)

In an attempt to improve the energy efficiency by bringing continuity in phase, we formulate Q^2PSK signal in six dimensional signal space. In general, the Q^2PSK signal can be written as

$$s(t) = A(t) \cos(2\pi f_c t + \theta(t)) \quad (5.5)$$

where $A(t)$ is the amplitude of the modulated carrier and $\theta(t)$ is the phase given by

$$\theta(t) = \tan^{-1} \left[\frac{\sum_{i=1}^n b_i(t) p_i(t)}{\sum_{i=1}^n a_i(t) p_i(t)} \right]. \quad (5.6)$$

We assume the data shaping components $p_i(t)$ are continuous for all t and the modulated signal maintains continuity in phase at every symbol transition instant; this is desirable for faster asymptotic fall off in the spectral density of the modulated signal. This condition is satisfied if

$$p_i((2k+1)T/2) = 0 \quad (5.7)$$

for all k . The minimum bandwidth solution for $p_i(t)$ is a sinc function which occupies a bandwidth of $1/4T$. But the minimum bandwidth solution being unique, one cannot have more than one $p_i(t)$ which maintain orthogonality condition (5.2) and occupy the same minimum bandwidth $1/4T$ at the same time. So different (non optimum) sets of shaping components are considered and their spectral efficiencies compared. One choice is a truncated sine function given by

$$\begin{aligned}
 x(t;T) &= A \frac{\sin(2\pi t/T)}{2\pi t/T} & |t| \leq \frac{T}{2} \\
 &= 0 & |t| > \frac{T}{2}
 \end{aligned} \tag{5.8}$$

where $A = 1.0518$ is a normalizing constant to make $x(t;T)$ a unit energy pulse. In order to maintain orthogonality among the data shaping components we constructed the set $\{ p_i(t) \}$ as follows :

$$p_1(t) = x(t;T) \tag{5.9a}$$

$$p_2(t) = (D_2^{-1} - D_2^{-1}) x(t;T/2) \tag{5.9b}$$

$$p_3(t) = (-D_3^{-1} + 1 - D_3^{-1}) x(t;T/3) \tag{5.9c}$$

*

$$p_{n-1}(t) = \sum_{k=1}^m \left((-1)^k D_n^{-k} + (-1)^{(k-1)} D_n^{-k} \right) x(t;T/n) \tag{5.9n-1}$$

$$p_n(t) = \sum_{k=-m}^m (-1)^k D_n^{-k} x(t;T/n) \tag{5.9n}$$

where $n=2m+1$ is an odd integer and the operator D_t^{-k} represents a delay of kT/n units of time. The construction of this set of data shaping components is illustrated in Figure 5.1.

Generation of sophisticated data pulse at high frequency (such as a truncated sine pulse at several hundred MHz) may become very expensive. So other choices of data shaping components which are less expensive are worth mentioning.

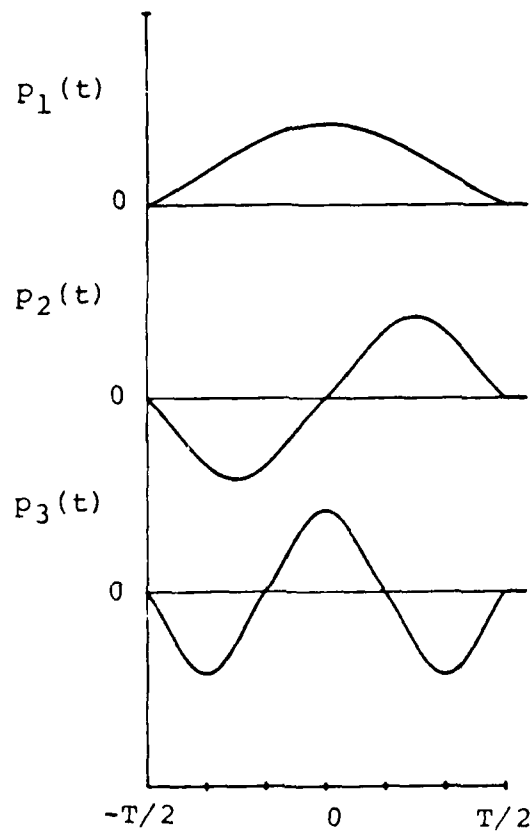


Figure 5.1. Truncated Sinc function data shaping components for Q^2PSK ($n=3$).

We consider the following set of three signals as an example

$$p_1(t) = \frac{2}{\sqrt{T}} \cos(\pi t/T) \cos(2\pi t/T) \quad (5.10a)$$

$$p_2(t) = \frac{2}{\sqrt{T}} \sin(\pi t/T) \sin(2\pi t/T) \quad (5.10b)$$

$$p_3(t) = \frac{2}{\sqrt{T}} \cos(\pi t/T) \sin(2\pi t/T) . \quad (5.10c)$$

This set of data shaping components satisfy both the orthogonal and zero crossing condition given by (5.2) and (5.7) respectively. Each of these signals can be expressed as the sum or difference of two signals of frequencies $f_1=1/2T$ and $f_2=3/2T$, so we call (5.9) composite waveforms.

The difference between the two frequencies is $1/T$; this is exactly twice the minimum spacing ($1/2T$) that one needs for coherent orthogonality of two FSK signals of duration T . So there must be another set of three signals with frequencies f_1, f_2, f_3 such that the difference between adjacent consecutive frequencies is the minimum spacing needed for minimum shift keying. This set is given by

$$p_1(t) = \sqrt{\frac{2}{T}} \cos(\pi t/T) \quad (5.11a)$$

$$p_2(t) = \sqrt{\frac{2}{T}} \sin(2\pi t/T) \quad (5.11b)$$

$$p_3(t) = \sqrt{\frac{2}{T}} \cos(3\pi t/T) . \quad (5.11c)$$

We call (5.11) simple wave forms. The set constructed from truncated sinc function becomes identical to this set of simple wave forms if one redefines $x(v;T)$ in (5.8) as $\cos(\pi v/T)$. The effect of modulating this set of simple data shaping components by orthogonal carriers is to translate the spectrum of a set of minimum

shift keying type signals (which is different from the well known MSK scheme) from baseband to a bandpass region. This is the basic difference between Quadrature-Quadrature Phase Shift Keying and Minimum Shift Keying which enables Q^2PSK to use a given bandwidth more efficiently in the bandpass region.

Next we will discuss the spectral properties of Q^2PSK schemes which utilize the set of truncated sinc pulses, composite waveforms and simple waveforms as the baseband data shaping components. Among these three sets of data shaping components, particularly the last two are favourable from an implementation view point; this is because they could be constructed by simple addition and subtraction of sinusoids which can be generated with perfection even at several hundred MHz frequency.

5.4 Spectral Density

The equivalent normalized baseband power spectral density of generalized Q^2PSK signal is given by,

$$S_{q^2psk}(f) = \frac{1}{n} \sum_{i=1}^n |P_i(f)|^2 \quad (5.12)$$

where $P_i(f)$ is the Fourier transform of the i^{th} data shaping pulse $p_i(t)$ and

$$\int_{-\infty}^{\infty} S_{q^2psk}(f) df = 1 .$$

Simple Wave Shape

The baseband data shaping components over $|t| \leq T/2$ are given by (5.11); the corresponding Fourier transforms are

$$P_1(f) = \frac{2\sqrt{2T}}{\pi} \left(\frac{\cos \pi f T}{1-4f^2 T^2} \right) \quad (5.13a)$$

$$P_2(f) = -j \frac{\sqrt{2T}}{\pi} \left(\frac{\sin \pi f T}{1-f^2 T^2} \right) \quad (5.13b)$$

$$P_3(f) = -6 \frac{\sqrt{2T}}{\pi} \left(\frac{\cos \pi f T}{9-4f^2 T^2} \right). \quad (5.13c)$$

Hence the spectral density is given by

$$S^s_{q^2_{pek}}(f) = \frac{T}{3\pi^2} \left(\frac{8\cos^2 \pi f T}{(1-4f^2 T^2)^2} + \frac{72\cos^2 \pi f T}{(9-4f^2 T^2)^2} + \frac{2\sin^2 \pi f T}{(1-f^2 T^2)^2} \right) \quad (5.14)$$

where the superscript s implies simple wave shaping.

Composite Wave Shape

The baseband data shaping components over $|t| \leq T/2$ are given by (5.10); the corresponding Fourier transforms are given by

$$P_1(f) = \frac{2\sqrt{T}}{\pi} \cos \pi f T \left(\frac{1}{1-4f^2 T^2} - \frac{3}{9-4f^2 T^2} \right) \quad (5.15a)$$

$$P_2(f) = \frac{2\sqrt{T}}{\pi} \cos \pi f T \left(\frac{1}{1-4f^2 T^2} + \frac{3}{9-4f^2 T^2} \right) \quad (5.15b)$$

$$P_3(f) = j \frac{2\sqrt{T}}{\pi} \cos \pi f T \left(\frac{2f T}{9-4f^2 T^2} - \frac{2f T}{1-4f^2 T^2} \right). \quad (5.15c)$$

Hence the spectral density is given by

$$S^c_{q^2_{pek}}(f) = \frac{8T}{3\pi^2} \cos^2 \pi f T \left(\frac{1+2f^2 T^2}{(1-4f^2 T^2)^2} + \frac{9+2f^2 T^2}{(9-4f^2 T^2)^2} + \frac{4f^2 T^2}{(9-4f^2 T^2)(1-4f^2 T^2)} \right) \quad (5.16)$$

where the additional superscript c stands to mean composite wave shaping.

Truncated Sinc Function Wave Shape

The data shaping components are given by (5.9); we consider only the first three components to form a six dimensional signal space. There is no closed form expression for the power spectral density; results due to numerical calculation are illustrated in Figures 5.2 and 5.3.

Figure 5.2 shows the power spectral densities of MSK and three continuous phase Q^2PSK cases; power spectral densities have been plotted against normalized frequency f/R_b , where R_b is the bit rate associated with respective schemes. It should be noted that the spectrum fall-off associated with all three generalized Q^2PSK schemes, each of which maintains continuity in phase, is much faster than that associated with MSK, although MSK also maintains a continuity in the carrier phase. Among three generalized Q^2PSK schemes, simple and composite wave shaping exhibit almost identical spectral density (except a few nulls in the composite case) which fall off somewhat faster than that of truncated sinc wave shaping. However, looking at the power spectral densities does not give any quantitative information about spectral compactness and energy efficiencies of the schemes.

A measure of spectral compactness is the percent of total power captured in a specified bandwidth; this is plotted in Figure 5.3 for all three schemes, where W represents one sided bandwidth around the carrier frequency. We consider ninety nine percent power bandwidth as the inverse measure of spectral compactness. Figure 5.3 shows that both simple and composite wave shaping schemes reach the ninety nine percent value at $W = 0.5R_b$ and at $W = 0.7R_b$ respectively.

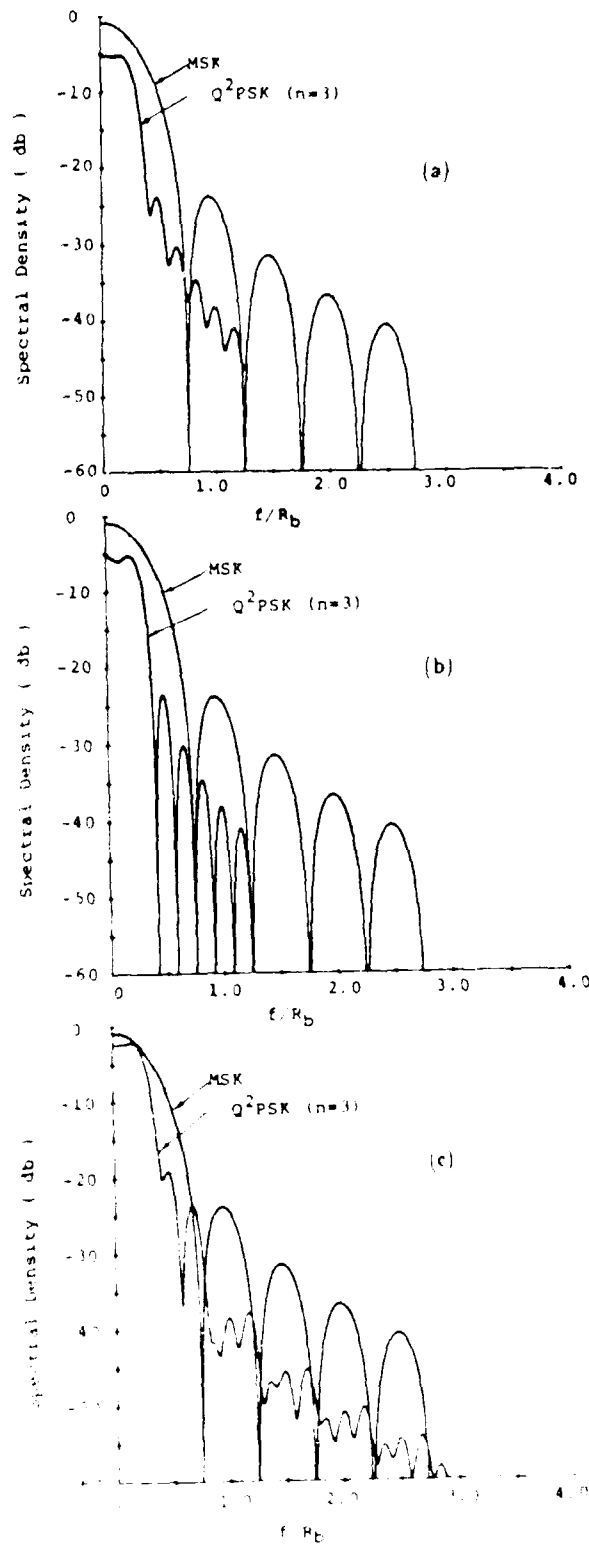


Figure 3.2 Spectral densities of MSK signal and Q^2PSK signals using (a) simple (b) composite and (c) Truncated Sinc function wave shapings

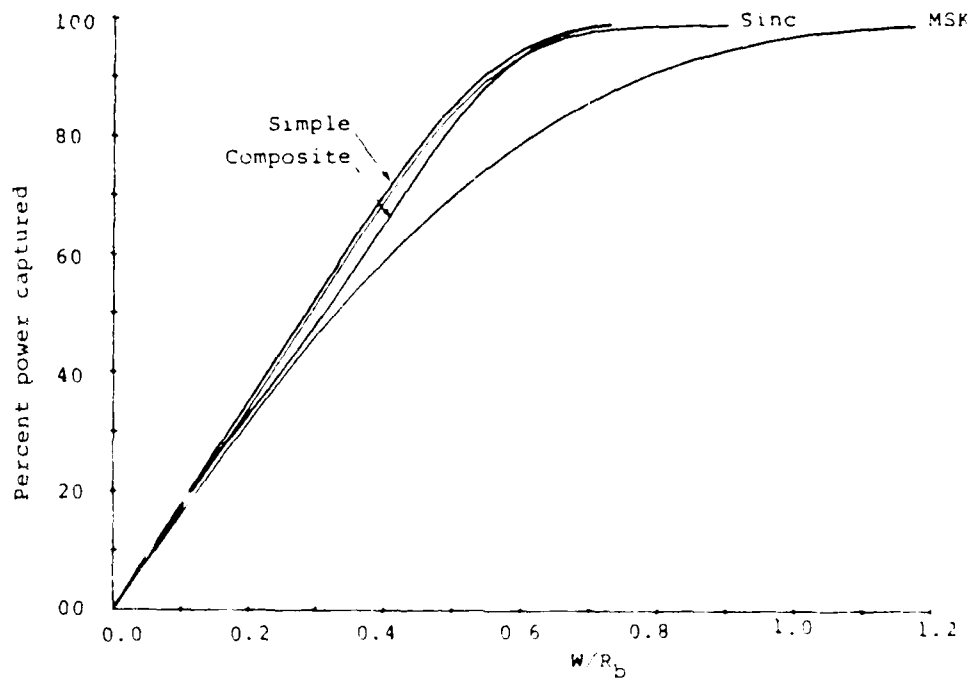


Figure 5.3. Percent power captured as function of bandwidth for MSK and Q^2 PSK ($n=3$) using truncated Sinc, Simple and Composite wave shapings.

respectively; whereas truncated sine wave shaping and MSK reach that value at $W = 0.9R_b$ and $W = 1.2R_b$ respectively. Therefore in an increasing order of spectral compactness, the four schemes come in the following order: MSK, $Q^2PSK(n=3)$, Truncated Sine wave shape, Simple and Composite wave shapes. The corresponding bandwidth efficiencies, defined to be the ratio of bit rate to bandwidth, are 0.83, 1.1, 1.33 and 1.38 respectively. Thus with composite wave shaping it is possible to achieve a bandwidth efficiency which is 1.65 times that of MSK. It should be remembered that $Q^2PSK(n=2)$ increases the bandwidth efficiency by a factor of two over MSK. Comparing Q^2PSK at $n=3$ to $n=2$, there is a loss of 35% in bandwidth efficiency; the gain is the continuity in phase which results in faster asymptotic spectrum fall-off.

In an attempt to compensate for this loss one may add a fourth data shaping component $p_4(t)$ to the set defined in (5.10) for the composite wave shaping, where the fourth component is given by

$$p_4(t) = \frac{2}{\sqrt{T}} \sin(\pi t/T) \cos(2\pi t/T). \quad (5.17)$$

It should be noted that this fourth component maintains orthogonality with respect to the three other components given in (5.10); but $p_4(\pm T/2) = \pm 1$ and therefore it will disrupt the continuity in phase. The Fourier transform of this data shaping component is given by

$$P_4(f) = j \frac{2\sqrt{T}}{\pi} \cos \pi f T \left[\frac{2fT}{9-4f^2T^2} + \frac{2fT}{1-4f^2T^2} \right]. \quad (5.18)$$

Hence the spectral density of the Q^2PSK signal which uses the set of four signals given by (5.10) and (5.17) as the data-shaping components is given by

$$S_{Q^2PSK}(f) = \frac{8T}{4\pi^2} \cos^2 \pi f T \left[\frac{1 + 4f^2 T^2}{(1 - 4f^2 T^2)^2} + \frac{9 + 4f^2 T^2}{(9 - 4f^2 T^2)^2} \right] \quad (5.19)$$

where the additional superscript *cnc* stands to mean composite but non continuous wave shaping. This spectral density has been studied along with that of continuous phase $n = 3$ case. Compared to the continuous phase case, the secondary sidelobes in this $n = 4$ situation are considerably higher in strength; the corresponding ninety nine percent power bandwidth is far above the $W_{99} = 0.725R_b$ value of $n = 3$ continuous phase case. This is due to abrupt discontinuities in the fourth data-shaping component $s_4(t)$ introduced into the new set. With a bandwidth equal to $0.725R_b$, the $n = 4$ case captures only 95.5% of the total spectral power. Hence addition of the fourth data-shaping component seems to be of no use.

If transmission is allowed over 99% power bandwidth of respective modulation schemes, one may reasonably assume that there will be no noticeable intersymbol interference and the hypercube geometry of the signal will virtually remain unchanged. Hence for Q^2PSK $n = 3$ schemes with bandwidth equal to $0.725R_b$ and $0.75R_b$ respectively for composite and simple wave shaping, the average bit energy requirement (E_b/N_0) is 9.6 dB. One may summarize all the results in the following table.

TABLE 5.1

**Energy and Bandwidth Efficiencies
of MSK, Q^2PSK and Generalized Q^2PSK**

Type of modulation	MSK biorthogonal	$Q^2PSK(n=3)$ trun.sinc	$Q^2PSK(n=3)$ simple	$Q^2PSK(n=3)$ composite	Q^2PSK $n=2$
Bandwidth efficiency	.83	1.11	1.33	1.38	1.66
E_b/N_0 for $P_b(E)=10^{-5}$	9.6dB	9.6dB	9.6dB	9.6dB	11.2dB

Q^2PSK performance has also been compared with that of QORC, a non constant envelope scheme [ref. to Section 2.3]. Though spectral density of QORC falls off as f^{-6} , while that of Q^2PSK as f^{-4} , the latter scheme outperforms the former in bandwidth efficiency. Bit error probability of Q^2PSK (simple), MSK and QORC are plotted in Figure 5.4 as functions of E_b/N_0 . This result is based on bandlimiting using a sixth order Butterworth filter with half power bandwidths $W=R_b$ for both MSK and QORC, $W=2/3R_b$ for Q^2PSK . Two different receivers have been considered for QORC (ref. to Section 2.3) : one is MSK, the other is QPSK. It is observed that the bit error rate performances of Q^2PSK and QORC (with MSK receiver) are almost identical; while energy efficiency (ie E_b/N_0 for a $P_b(E)=10^{-5}$) of MSK is slightly better by 0.4 dB. However, for the same transmission bandwidth, transmission rate in Q^2PSK is 1.5 times that in QORC and MSK.

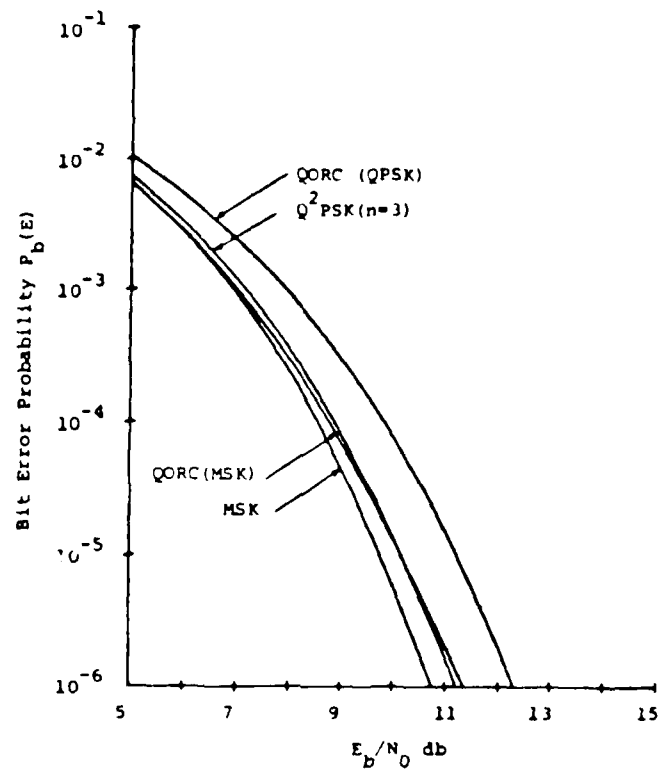


Figure 5.4. Bit error probabilities as functions of E_b/N_0 for Q^2PSK (simple wave shape), MSK and QORC signals.

5.5 Summary

In applications where bandwidth efficiency is of primary concern, Q^2PSK ($n = 2$) seems to be a better candidate. $Q^2PSK(n = 3)$ may find a suitable position where energy efficiency is more important or use of line filtering (bandlimiting) is cost prohibitive.

CHAPTER SIX

PULSE SHAPING AND NYQUIST RATE

6.1 Introduction

It is known that the best achievable rate with a zero memory modulation is the Nyquist rate $\frac{1}{2}$ of two symbols per second per Hertz. For binary or two level communication, the rate is two bits per second per Hertz. This rate is achievable only with the use of sinc function as the data shaping pulse. But realization of sinc function is known to have problems from implementation points of view. In practice, the problem is reduced by allowing a bandwidth in excess of Nyquist's minimum bandwidth, which is half the symbol (or bit) rate. But the use of excess bandwidth lowers the bandwidth efficiency below the theoretical limit of two.

Lender [3.6.12] pointed out that if one neglects Nyquist's assumption of zero memory of the system, the two symbols (or bits) per second per Hertz rate can be achieved with practical filter shapes. He introduced a correlative coding, known as Duobinary coding, which needs three level detection at the receiver. The three level detection increases complexity in the receiver and suffers a 3dB loss in the bit error rate performance over the Nyquist's proposed scheme. Above all, it does not maintain binary detection.

Like Nyquist's and Fender's schemes, Q^2PSK makes two parallel transmissions on each carrier and like Fender's, it maintains binary detection. Q^2PSK as discussed in chapter three, uses a half-cosinusoid and a half-sinusoid as two data shaping pulses. These pulses are practically realizable. After bandlimiting, however, these two pulses cause intersymbol interference and therefore Q^2PSK requires higher bit energy compared to Nyquist's sinc pulse scheme. Its bandwidth efficiency is 1.66, close to but lower than the Nyquist's efficiency of two. In an attempt to eliminate both in-phase and cross-intersymbol interference in Q^2PSK transmission, a new class of pulse shapes is suggested. A few members of this class (with minor modification) are convenient for implementation and achieve the Nyquist's rate of two bits per second per Hertz using binary detection. Its bit energy expenditure is less than that of Duobinary.

6.2 Pulse Shaping

The original Q^2PSK used a half-cosinusoid and a half-sinusoid (defined as $p_1(t)$ and $p_2(t)$ in 3.2a and 3.2b) as two data shaping pulses. It is observed that in achieving twice the bandwidth efficiency of minimum shift keying, the original Q^2PSK requires about 1.6 dB increase in the average bit energy which is mostly due to intersymbol interference caused by the bandlimiting effect on the data shaping pulse $p_2(t)$. With the ninety-nine percent power bandwidth ($W = 1.2/T$) of MSK as the definition of channel bandwidth, a data pulse of the shape $p_1(t)$ gets through almost undistorted; but a data pulse of the shape $p_2(t)$ is seriously distorted because of the sharp discontinuities in $p_2(t)$ at $t = \pm T$. It is also

observed that if three or more pulses of the shape $p_2(t)$ occur in a row with the same polarity then bandlimiting causes a destructive interference of the worst kind. This worst case situation of interference is primarily responsible for the requirement of higher bit energy. In an attempt to improve the energy efficiency, one way of reducing the intersymbol interference is by applying proper wave shaping to the data pulses. In other words, one needs to find suitable shapes $p_1(t)$ and $p_2(t)$ so that their effect of intersymbol interference due to bandlimiting is either eliminated completely or reduced greatly.

In this section we look into Q^2PSK transmission in the baseband domain. The baseband model of the transmitter and receiver is illustrated in Figure 6.1. (In an actual situation, however, two such blocks of transmitter and receiver are present; one is associated with the sine carrier, the other is with the cosine carrier.) In this model the input binary data stream has been represented by a series of impulses occurring at intervals of T sec. The amplitude factor a_k can be either $+1$ or -1 . The input stream is demultiplexed into two streams; the rate of impulses in the demultiplexed streams is half the rate ($1/T$) in the incoming stream. $P_1(f)$ and $P_2(f)$ are the pair of transmitter filters; $P_1'(f)$ and $P_2'(f)$ are the corresponding matched filters at the receiver. The receiver and transmitter filters occupy a common bandwidth $(-W, W)$. In absence of noise $n(t)$, the signal at the input of receiver is given by,

$$s_{Q^2PSK}(t) = \sum_{k=-\infty}^{\infty} (a_{1,k} p_1(t-2kT) + a_{2,k} p_2(t-2kT)) \quad (6.1)$$

where $p_1(t)$ and $p_2(t)$ are the impulse responses of the transmitter filters which are

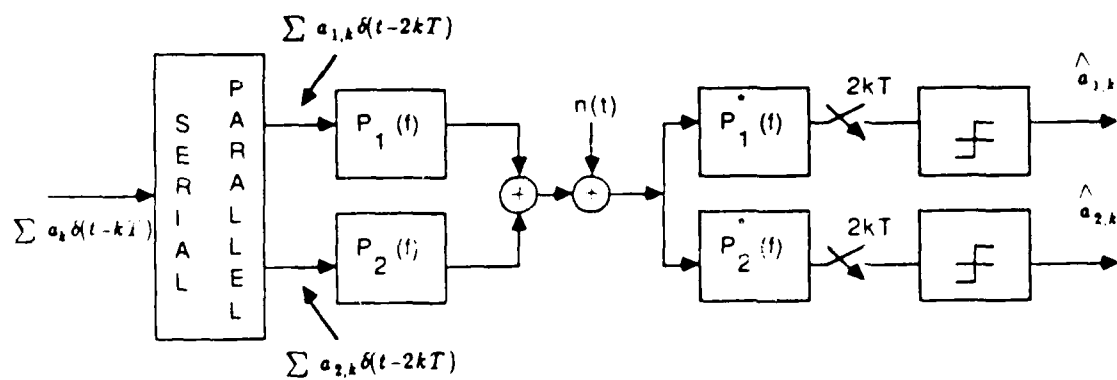


Figure 6.1. Baseband model of Q^2PSK transmitter and receiver.

not necessarily time limited (unlike the original Q^2PSK data pulses) and the $a_{i,k}'$'s being either +1 or -1 represent the demultiplexed information bits over the interval $(k-1)T < t < (k+1)T$.

At the receiver the matched filter outputs are sampled at regular intervals of $2T$ and binary decisions are taken using a threshold detector with the threshold set at zero. The sampled values at the output of the two matched filters represent the coordinates of the baseband signal in a two dimensional signal space where $p_1(t)$ and $p_2(t)$ serve as the bases. Suppose the two observation bits are $a_{1,0}$ and $a_{2,0}$. The coordinate values are given by

$$x_{10} = a_{1,0} R_{11}(0) + \sum_{n \neq 0} a_{1,n} R_{11}(n) + \sum_n a_{2,n} R_{21}(n) \quad (6.2)$$

$$x_{20} = a_{2,0} R_{22}(0) + \sum_{n \neq 0} a_{2,n} R_{22}(n) + \sum_n a_{1,n} R_{12}(n) \quad (6.3)$$

where,

$$R_{11}(n) = R_{11}(2nT) = \int_{-T}^T p_1(t-2nT) p_1(t) dt \quad (6.4)$$

$$R_{22}(n) = R_{22}(2nT) = \int_{-T}^T p_2(t-2nT) p_2(t) dt \quad (6.5)$$

$$R_{12}(n) = R_{12}(2nT) = \int_{-T}^T p_1(t-2nT) p_2(t) dt \quad (6.6)$$

$$R_{21}(n) = R_{21}(2nT) = \int_{-T}^T p_2(t-2nT) p_1(t) dt \quad (6.7)$$

are the sampled values of the auto and cross-correlation function of the pulses $p_1(t)$ and $p_2(t)$. The first term on the right of (6.2) or (6.3) is the desired one ; the remaining two summation terms are due to intersymbol interference. It is to be noted that $p_1(t)$ and $p_2(t)$, in general, are not timelimited; so both stream of

pulses are causing intersymbol interference. To eliminate the effect of ISI in the process of making binary decisions one needs the following criterion

$$R_{11}(n) = R_{22}(n) = \delta_{n0} \quad (6.8a)$$

$$R_{12}(n) = R_{21}(n) = 0 \quad (6.8b)$$

where,

$$\begin{aligned} \delta_{n0} &= 1 & n &= 0 \\ &= 0 & n &\neq 0. \end{aligned}$$

It should be observed that the above set of criterion imposes much stronger restrictions on the shape of the two data pulses than the Nyquist criterion [2.25] or simple orthogonality between the two pulses. The auto and cross-correlation functions are related to the pulse spectra by the following relations :

$$R_{kk}(n) = \int_{-\infty}^{\infty} P_k^*(f) P_k(f) e^{j4n\pi f T} df \quad (6.9)$$

$$R_{kl}(n) = \int_{-\infty}^{\infty} P_k^*(f) P_l(f) e^{j4n\pi f T} df \quad (6.10)$$

$$k, l = 1, 2; k \neq l.$$

Now, $R_{kk}(n)$ can be written in the following form

$$R_{kk}(n) = \sum_m \int_{\frac{2m-1}{4T}}^{\frac{2m+1}{4T}} P_k^*(f) P_k(f) e^{j4n\pi f T} df. \quad (6.11)$$

A change of variables and an interchange of summation and integration gives (6.8a) as

$$R_{kk}(n) = \int_{-\frac{1}{4T}}^{\frac{1}{4T}} S_{kk}^*(f) e^{j4n\pi f T} df = \delta_{n0} \quad (6.12)$$

where,

$$S_{k,q}^*(f) = \sum_m P_k(f + \frac{m}{2T}) e^{j\frac{m}{4T}}, \quad f \in [-\frac{1}{4T}, \frac{1}{4T}]$$

$$= 0, \quad f \notin [-\frac{1}{4T}, \frac{1}{4T}] \quad (6.13)$$

is the equivalent wrapped version of the bandlimited power spectrum of the k^{th} pulse $p_k(t)$. Similarly (6.8b) can be written as

$$R_u(\tau) = \int_{-\frac{1}{4T}}^{\frac{1}{4T}} S_{k,q}^u(f) e^{j2\pi f\tau} df = 0 \quad (6.14)$$

where,

$$S_{k,q}^u(f) = \sum_m P_k^*(f + \frac{m}{2T}) P_l(f + \frac{m}{2T}) e^{j\frac{m}{4T}}, \quad f \in [-\frac{1}{4T}, \frac{1}{4T}]$$

$$= 0, \quad f \notin [-\frac{1}{4T}, \frac{1}{4T}] \quad (6.15)$$

is the equivalent wrapped version of the bandlimited cross power spectrum of the pulses $p_k(t)$ and $p_l(t)$. The equivalent wrapped version is constructed by slicing the original spectrum into segments of width $1/2T$ and superimposing all the segments on the interval $[-1/4T, 1/4T]$.

In an attempt to improve the energy efficiency of QPSK, we, therefore, frame the following guidelines to study the scope of wave shaping in reducing the effect of ISI:

Choose $P_k(f)$, $k = 1, 2$ such that

$$\int_{-\frac{1}{4T}}^{\frac{1}{4T}} S_{k,q}^*(f) e^{j2\pi f\tau} df = 0, \quad \tau \neq 0 \quad (6.16)$$

and

$$\int_{-\infty}^{\infty} S_{eq}^{(k)}(f) e^{j4\pi k f T} df = 0 \quad (6.16b)$$

$$k = 1, 2; \quad k \neq i$$

are satisfied for complete elimination of ISI, or the above two integrals are minimized so that the effect of ISI is minimized in the sense of minimizing the mean square of error.

6.3 Solutions to Pulse Shaping Problem

There are infinite number of solutions for $P_1(f)$ and $P_2(f)$ which satisfy both (6.14) and (6.16). A few of them are illustrated in Figure 6.2. The figure pair (a) and (b) is a Hilbert Transform pair. This pair achieves the same purpose as the filter pair (6.1) and (6.2). At the same time, it also faces all the realization problems which (6.1) and (6.2) face. Besides, a Hilbert Transform pair is not a causal system because of the finite dc content. The filter pair (c) and (d) is a causal system because of the finite dc content. The filter pair (e) and (f) is a causal system because of the finite dc content but it has the old problem of infinite side lobes.

Figure 6.2. Four filter pairs

The filter pair (a) and (b) illustrated in Figure 6.2c is a Hilbert Transform pair. The filter pair (c) and (d) is a causal system because of the finite dc content. The filter pair (e) and (f) is a causal system because of the finite dc content but it has the old problem of infinite side lobes. As the filter pair (a) and (b) is a Hilbert Transform pair, the filter pair (c) and (d) is a Hilbert Transform pair. As the filter pair (e) and (f) is a causal system because of the finite dc content, the filter pair (g) and (h) is a causal system because of the finite dc content.

The filter pair (a) and (b)

AD-A185 838

QUADRATURE-QUADRATURE PHASE SHIFT KEYING(U) HIGHWAY
UNIV ANN ARBOR COMMUNICATIONS AND SIGNAL PROCESSING LAB
D SARA SEP 86 021779-3-T N00014-84-K-0066

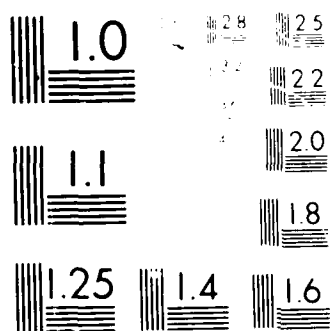
2/2

UNCLASSIFIED

F/B 25/5

NL





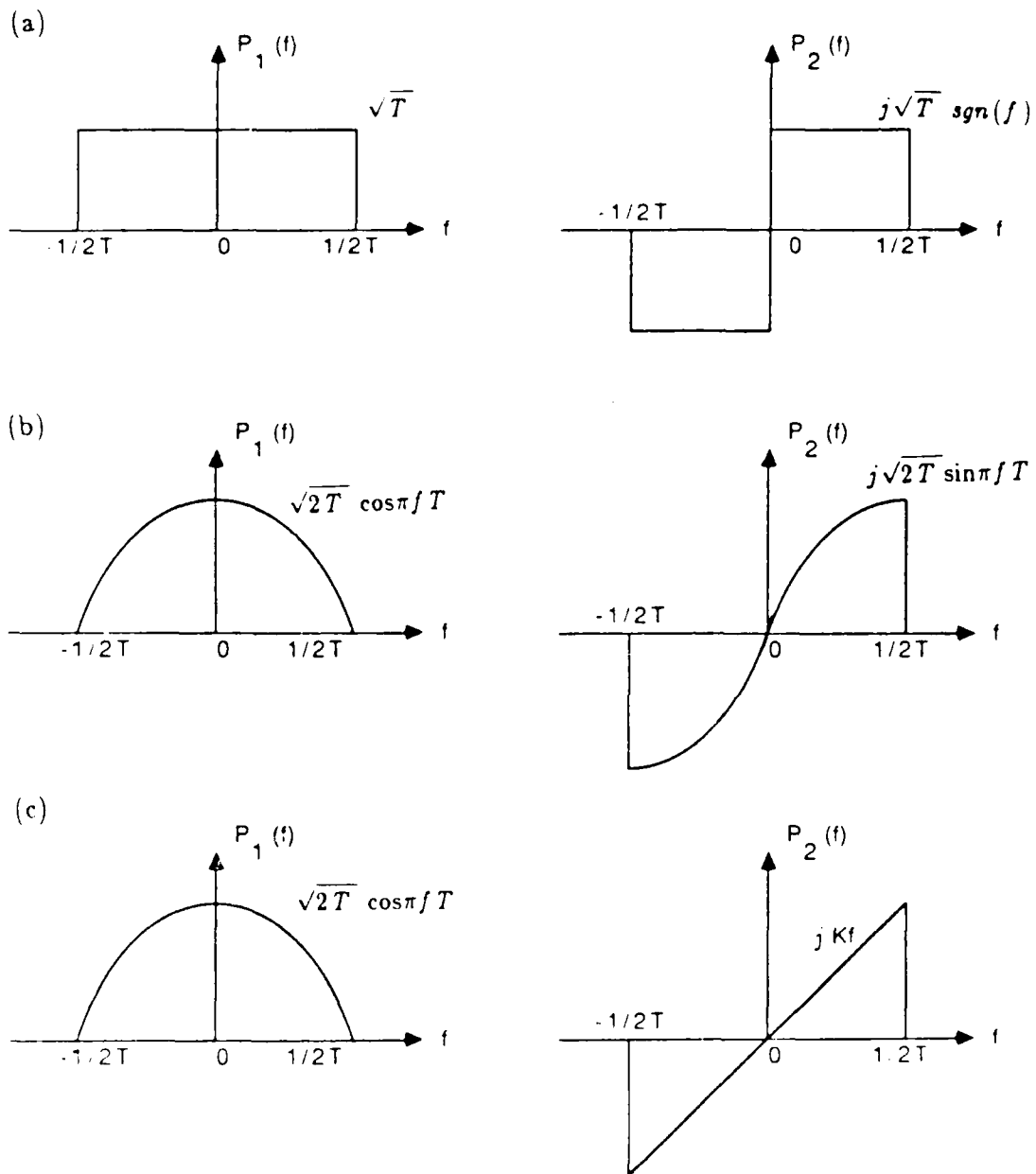


Figure 6.2. Transmitter filter pairs for Q^2PSK transmitter with zero inphase and zero cross intersymbol interference.

However, instead of sharp cut off filtering at $f = \pm \frac{1}{2T}$ if one allows a Butterworth filtering alongwith an ideal differentiator, the realization problem is greatly reduced. The bit error rate performance has been studied for $P_1(f) = \sqrt{2T} \cos \pi f T$ and $P_2(f) = fB(f)$, where $B(f)$ is a Butterworth low pass filter of second order with three dB bandwidth as $W = 0.5 R_b$. The corresponding transfer function is given by,

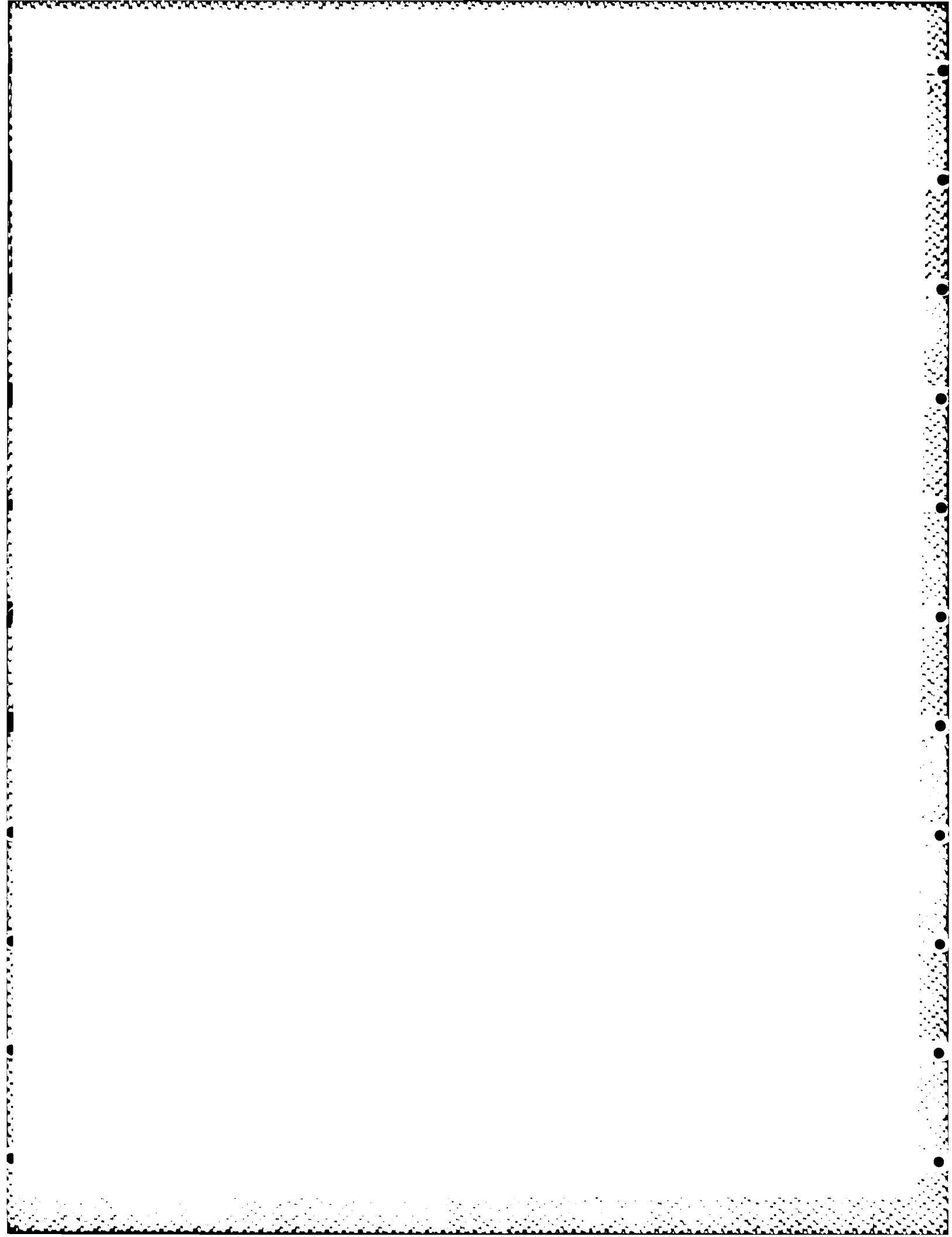
$$P_2(s) = \frac{s}{s^2 + \sqrt{2}s + 1} \quad (6.17)$$

where s is the complex frequency (normalized with respect to 3 dB bandwidth). This is a realizable transfer function. The corresponding bandwidth efficiency is substantially higher than that of the original version of Q^2PSK . The energy efficiency is also improved from 11.2 dB to 10.8 dB. Thus pulse shaping provides improvement in both energy and bandwidth efficiencies over the original Q^2PSK . If, however, the bandwidth of the Butterworth filter is reduced from $0.5 R_b$ to $0.4 R_b$, the bandwidth efficiency is increased from 2.0 to 2.5. The energy efficiency in this situation is 12.7 dB. This energy efficiency is comparable to the 12.6 dB value of Lender's Duobinary scheme, although the Q^2PSK transmission rate in this situation is higher than the Duobinary rate. And above all, a noticeable advantage of Q^2PSK over Duobinary is its binary detection at the receiver. It is noteworthy that Q^2PSK assumes a zero memory transmission while Duobinary signal exploits the advantage of correlative coding on Nyquist's minimum bandwidth zero memory signal. So the introduction of some sort of memory in

Q^2PSK format through the use of correlative coding may turn out to be quite interesting and remains an open problem.

6.4 Summary

Pulse shapes which are optimum for Q^2PSK transmission are derived. The optimality of this class of pulse shapes lies in zero in-phase and zero cross intersymbol interference. A few members of this class are convenient from a realization point of view and achieve the limit of two bits per second per Hertz using binary detection. Bit energy expenditure and system complexity are reduced compared to the Duobinary scheme, which uses three level detection.



CHAPTER SEVEN

CONCLUDING REMARKS

7.1 Thesis Summary

Quadrature-Quadrature phase shift keying (Q^2PSK) is a new spectrally efficient modulation scheme which can be considered as two minimum shift keying type signalling schemes in parallel. It uses two data shaping pulses and two carriers which are pairwise quadrature in phase; the scheme thus utilizes available signal space dimensions in an efficient way to increase the bandwidth efficiency by a factor of two over two dimensional schemes such as QPSK, MSK, TFM. The bit error rate performance, however, depends on the choice of the data shaping pulse pair. With simple cosinusoidal and sinusoidal data shaping pulses the E_b/N_0 requirement is approximately 1.6 dB higher than that of MSK and 0.6 dB higher than that of TFM. With the suboptimum pulse shapes discussed in chapter six, the bit error rate performance of Q^2PSK becomes closer to that of MSK, though for a given bandwidth the transmission rate in Q^2PSK remains twice the rate in MSK.

Quadrature-Quadrature Phase Shift Keying, unlike MSK and TFM, does not maintain a constant envelope, which is desirable for certain non linear channels. However, a simple parity check coding on Q^2PSK format with cosinusoidal and sinusoidal pulses as data shaping components forms a constant envelope signal.

The bandwidth efficiency of this coded Q^2PSK is 1.5 times that of MSK and TFM. The receiver based on the assumption of bit by bit detection has been considered; the bit error rate performance of this coded scheme is about 0.3 dB better than that of TFM while 0.7 dB worse than MSK. However, with symbol by symbol detection the bit error rate performance is expected to be much better than that of MSK; this is because the Euclidean distances among the signal points in the coded Q^2PSK format is higher than that in MSK.

Like MSK, Q^2PSK also has self synchronizing and self clocking ability. A synchronization scheme which recovers carrier phase and bit timing information is presented for coherent demodulation of the Q^2PSK signal. Due to the coding effect, this synchronization scheme does not work for the coded Q^2PSK ; a similar but different synchronization scheme is presented for coherent demodulation of coded Q^2PSK signal.

The original Q^2PSK uses two data shaping pulses and two carriers which are pairwise quadrature in phase. The scheme is generalized by incorporating n number of orthogonal data shaping pulses alongwith two orthogonal carriers to create a $2n$ -dimensional signal space. The original case of $n=2$ increased the bandwidth efficiency by a factor of two over MSK at the expence of 1.6 dB increase in the average bit energy. The extra bit energy requirement is avoided by allowing a loss in the bandwidth efficiency; in the special case of $n=3$ a bandwidth efficiency which is 1.5 times that of MSK is achieved without any increase in the average bit energy. In applications where bandwidth efficiency is of primary concern and Q^2PSK ($n=2$) seems to be a better candidate; but where

energy efficiency is more important or use of fine filtering (bandlimiting) is cost prohibitive , $Q^2PSK(n=3)$ may find a suitable position.

The original Q^2PSK uses a half cosinusoid and a half sinusoid as two data shaping pulses. On bandlimiting, these two pulses cause intersymbol interference and therefore Q^2PSK requires a little higher bit energy compared to MSK. In an attempt to eliminate both in phase and cross intersymbol interference a new class of pulse shapes is suggested. A few members of this class are convenient from an implementation view point and improve both energy and bandwidth efficiencies considerably over the original scheme. With these pulse shapes, Q^2PSK achieves the Duobinary rate of two bits per second per Hertz using binary detection at the receiver while Duobinary needs three level detection and hence higher bit energy requirement.

7.2 Possible Future Developments

Constant Envelope in Multidimensional Space

Many of the constant envelope modulation schemes in the literature [3,4,8,10,23] , assume a two dimensional transmission. The development of constant envelope Q^2PSK showed that a four dimensional transmission achieves considerable higher spectral efficiency. In the two dimensional situation the tip of the modulated signal vector moves over a circle, while in Q^2PSK (coded) the tip moves over a hyper sphere of dimension four. In general, one may consider a constant envelope modulated signal as being one with a constellation of signal points lying on a hyper sphere in a multidimensional signal space. An attempt to

develop the theory of such multidimensional constant envelope modulation may bring a better understanding of the trade off between constant envelope and efficient use of bandwidth; it may also bring some spectral efficiency.

Correlative Coding on Q^2PSK

In the last decade, considerable research has been done on correlative coding. In many occasions it has been found to be effective in (i) achieving spectral efficiency [6,11] (ii) providing suitable spectral shaping [11] and (iii) designing a class of constant envelope signals [4,10,23]. Most of the results apply to one or two dimensional transmission. One may easily extend the usefulness of these results to higher dimensional transmission such as Q^2PSK .

In chapter six, we discussed optimum pulse shapes for Q^2PSK transmission. In deriving these pulse shapes we assumed a zero memory channel; in other words, we assumed signal levels to be independent over successive intervals. Some of the pulse shapes we discussed in this context suffer from realization problems. It is expected that application of correlative coding to these pulse shapes will ease the realization problem; at the same time it may improve the spectral efficiency.

Correlative coding has also been successfully applied to PSK systems in smoothing out the phase trajectories of the carrier. Such smoothing operation results in good power efficiency and low level out-of-band radiation. For example, when phase trajectories of an MSK signal is smoothed out by the use of correlative coding one gets TFM signal which is more spectrally compact than the MSK

signal. One may apply the same idea to the newly developed Q^2PSK signal and lower the out-of-band radiation.

Convolution Coding on Q^2PSK

With the present day technology, Viterbi decoding has become a practical and a powerful method for decoding convolutional codes and improving the energy efficiency over uncoded schemes by an amount of 4-6 dB [26]. This result applies to a wide variety of one and two dimensional transmission schemes. It has been found that with simple hand-designed trellis codes, coding gains of 3-4 dB can be achieved without any noticeable loss in the bandwidth efficiency [27]. The design procedure of this simple trellis code assumes that m bits of information are encoded per modulation interval so that there are 2^m possible transitions. An extended set of 2^{m+1} channel signals is considered and half of these channel signals are assigned to the 2^m possible transitions such as to achieve maximum Euclidean distance among the code words. After the development of Q^2PSK , it is an open problem to search for suitable trellis codes which may increase the free distance among the signal points in coded Q^2PSK type modulation. In addition to the coding gain, one may also expect to find a suitable set partitioning technique (on extended channel signals) which results in constant envelope signals.

APPENDICES

APPENDIX A

PROBABILITY DENSITY FUNCTION OF SIGNAL LEVEL

IN BANDLIMITED SITUATION

The bandlimited baseband Q^2PSK signal can be written as

$$s_{q^2psk}(t) = \sum_{k=-M}^M \left(a_{1,k} p_1(t-2kT) + a_{2,k} p_2(t-2kT) \right) + n(t) \quad -T < t < T \quad (A.1)$$

where $p_1(t)$ and $p_2(t)$ are the bandlimited data pulses extending over $-(2M+1)T$ to $(2M+1)T$, where M is an integer and $n(t)$ is the additive Gaussian noise with two sided spectral density as $N_0/2$. Here, $a_{1,k}$'s being either $+1$ or -1 represent the demultiplexed information bits over the interval $(k-1)T < t < (k+1)T$.

The receiver consists of two filters matched to $p_1(t)$ and $p_2(t)$. The matched filter outputs are sampled at regular intervals of $2T$ and binary decisions are taken using zero crossing detectors. The sampled values at the output of the two matched filters represent the coordinates of the received baseband signal in a two dimensional signal space where $p_1(t)$ and $p_2(t)$ serve as the bases. Suppose the two observation bits are a_{10} and a_{20} . The coordinates are given by the random variables X_{10} and X_{20} , where

$$X_{10} = a_{10} R_{11}(0) + \sum_{n \neq 0} a_{1,n} R_{11}(n) + \sum_{n \neq 0} a_{2,n} R_{12}(n) + N_1 \quad (A.2)$$

$$X_{20} = a_{20} R_{22}(0) + \sum_{n \neq 0} a_{2,n} R_{22}(n) + \sum_{n \neq 0} a_{1,n} R_{12}(n) + N_2 \quad (A.3)$$

Here $\eta_{ij}(t) = \eta_{ij}(t, \mathbf{x})$ is the noise correlation function of the process $\eta_{ij}(t)$ and $\eta_{ij}(t, \mathbf{x}) = \eta_{ij}(t, \mathbf{x} + \mathbf{b})$. N_1 and N_2 are zero mean Gaussian white noises with variances $\sigma_{N_1}^2 = \sigma_{N_2}^2 = \frac{1}{2} \int_{-\infty}^{\infty} \eta_{ij}(t) dt = 1$. One may write (A.2) and (A.3) as

$$X_{1,j}(t) = X_{1,j}(0) + N_{1,j}(t) + \sum_{i=1}^M \beta_{1i}(t) R_{1i}(t) + N_1 \quad (\text{A.4})$$

$$X_{2,j}(t) = X_{2,j}(0) + N_{2,j}(t) + \sum_{i=1}^M \beta_{2i}(t) R_{2i}(t) + N_2 \quad (\text{A.5})$$

where $X_{1,j}(0)$ and $X_{2,j}(0)$ are discrete random variables each of which may take one of the three values $\pm 2, 0, \pm 2$ with probability $1/4, 1/2$ and $1/4$ respectively. In order to compute the bit error probability $P_b(E)$, one needs to compute the signal-to-noise ratio in the absence of noise (given by the random variables,

$$S_{1,j} = X_{1,j} + N_1 \quad (\text{A.6})$$

$$S_{2,j} = X_{2,j} + N_2. \quad (\text{A.7})$$

The average bit error probability $P_b(E)$ can be computed from

$$P_b(E) = \frac{1}{2^{2M+1}} \sum_{\mathbf{x}} \left[Q \left(\sqrt{\frac{2s_{1,0}^2(\mathbf{x})}{N_0 R_1(0)}} \right) + Q \left(\sqrt{\frac{2s_{2,0}^2(\mathbf{x})}{N_0 R_2(0)}} \right) \right] \quad (\text{A.8})$$

where \mathbf{x} is indexed over 2^{2M+1} data combinations. In order to calculate $P_b(E)$ one needs to compute the signal levels and the corresponding probabilities of error in each of the 2^{2M+1} situations. The number of computations and the computing time increase exponentially with $2(2M+1)$. An alternative method lies in finding the probability density functions $p_{X_{1,j}}(x)$ and $p_{X_{2,j}}(x_{2,j})$ for the random variables

X_{10} and X_{20} and then calculating the bit error probability using the following relation

$$P_b(E) = \frac{1}{2} \int_{R_1(0)}^{\infty} f_{X_{10}}(x_{10}) dx_{10} + \frac{1}{2} \int_{R_2(0)}^{\infty} f_{X_{20}}(x_{20}) dx_{20}. \quad (\text{A.9})$$

In this method, computation effort increases only linearly with $2(2M+1)$.

Computation of pdf's

The characteristic function [18] of the random variable X_{10} is

$$\begin{aligned} \Phi_{X_{10}}(f) &= E \left(e^{j2\pi f X_{10}} \right) \\ &= e^{-2\pi^2 f^2 \sigma_1^2} \cdot \cos 2\pi f R_1(0) \cdot \prod_{i=1}^M \cos^2 2\pi f R_{11}(i) \cdot \prod_{i=1}^M \cos^2 2\pi f R_{21}(i). \end{aligned} \quad (\text{A.10})$$

Similarly,

$$\begin{aligned} \Phi_{X_{20}}(f) &= E \left(e^{j2\pi f X_{20}} \right) \\ &= e^{-2\pi^2 f^2 \sigma_2^2} \cdot \cos 2\pi f R_2(0) \cdot \prod_{i=1}^M \cos^2 2\pi f R_{22}(i) \cdot \prod_{i=1}^M \cos^2 2\pi f R_{12}(i). \end{aligned} \quad (\text{A.11})$$

The probability density functions $f_{X_{10}}(x_{10})$ and $f_{X_{20}}(x_{20})$ are given by the Fourier transforms of $\Phi_{X_{10}}(f)$ and $\Phi_{X_{20}}(f)$.

The bit error rate performances of Q^2PSK under bandlimited situation have been evaluated using the relations (A.9) through (A.11). The procedure lies in the following steps:

- (i) Compute the sampled auto and cross-correlation functions $R_{11}(k)$, $R_{12}(k)$, etc. of the bandlimited data pulses for $k = 0, 1, 2, 3, \dots$

(ii) Choose M and compute the sample points of $\Phi_{x_{10}}(f)$ and $\Phi_{x_{20}}(f)$ using (A.10) and (A.11) [typical selected set of parameters : $M = 10$ i.e. ISI from ten adjacent symbols on either side, Number of sampling points, $N = 1024$].

(iii) Take FFT of the set of sample points found in step (ii) for finding sampled values of $f_{x_{10}}(z_{10})$ and $f_{x_{20}}(z_{20})$ and then use (A.9) for computing the bit error probability $P_b(E)$.

This procedure has been followed in chapter three, four, five and six for evaluating the bit error rate performance of different signalling schemes under bandlimited situations in the presence of additive white Gaussian noise (AWGN). The key equations (A.9) through (A.11) used in the evaluations were modified according to the need of the situations involved. For example, with MSK or any two dimensional scheme, one need not consider the cross-correlation functions and the computational effort is reduced by half. Similarly, for $Q^2PSK(n=3)$, one needs modifying all of (A.9), (A.10) and (A.11) in order to include the effect of transmission due to the third pulse shaping component.

APPENDIX B

 Q^2PSK AND FOUR LEVEL MSK

The four level MSK scheme is similar to the conventional biorthogonal MSK scheme except the fact that here each pair of input information bits (each bit being of duration $T/2$) is first coded into one of the four possible levels $L_i, i = 1, 2, 3, 4$. The stream of coded levels (each level being of duration T) is then treated as the input to a conventional MSK modulator. So, the amplitude of the cosine shaped data pulses, as described in Figure 2.2, instead of being only $+1$ or -1 , takes one of the four values from the set $\{L_i\}_{i=1}^4$. Thus four level MSK accepts twice as many input bits as ordinary MSK. To minimize the average bit energy requirement for a given probability of error, the amplitude levels are assumed to be placed symmetrically around the origin as illustrated in Figure B.1. The optimum decision regions D_i for each level L_i are also shown. The coding has been performed in such a way that adjacent levels differ by one bit only; this will reduce the average bit error rate. If we maintain the 99% power bandwidth ($W = 1.2/T$) as the channel bandwidth, there will be no noticeable intersymbol interference. In that situation, the channel is completely defined by a set of probabilities $\{p_{ij}\}_{i,j=1}^4$ where p_{ij} is the probability that level L_i is transmitted and L_j is detected. The average bit error probability is given by,

$$P_b(E) = \frac{1}{4} \sum_{i=1}^4 P_{b_i} \quad (B.1)$$

where P_{b_i} is the bit error probability if only the i^{th} level were allowed to be

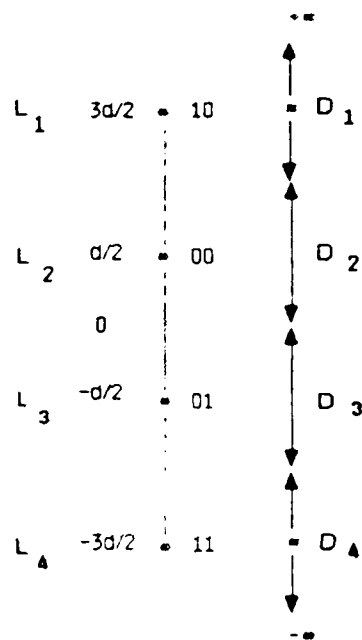


Figure B.1 Coding scheme for four-level MSK

transmitted. By trivial reasoning one may write

$$P_{b1} = \frac{1}{2} (p_{12} + 2p_{13} + p_{14}) \quad (\text{B.2})$$

$$P_{b2} = \frac{1}{2} (p_{21} + p_{23} + 2p_{24}) \quad (\text{B.3})$$

and by symmetry,

$$P_{b4} = P_{b1} \quad (\text{B.4})$$

$$P_{b3} = P_{b2} \quad (\text{B.5})$$

$$p_{12} = p_{23} \quad (\text{B.6})$$

Hence the average bit error probability is

$$P_b(E) = \frac{1}{4} (2p_{12} + 2p_{13} + 2p_{24} + p_{14} + p_{21}) \quad (\text{B.7})$$

Now referring to Figure B.1 and writing $n(t)$ for the additive Gaussian noise component,

$$\begin{aligned} p_{12} &= \text{Prob} \left[-\frac{d}{2} > n(t) > -\frac{3d}{2} \right] \\ &= Q \left(\frac{d/2}{\sqrt{N_0/2}} \right) - Q \left(\frac{3d/2}{\sqrt{N_0/2}} \right) \\ &= Q(r) - Q(3r) \end{aligned} \quad (\text{B.8})$$

where,

$$r = \sqrt{\frac{4E_b}{5N_0}}$$

and

$$E_b = \frac{5d^2}{8}$$

is the average bit energy.

Similarly,

$$p_{13} = Q(3r) - Q(5r) \quad (\text{B.9})$$

$$p_{14} = Q(5r) \quad (\text{B.10})$$

$$p_{21} = Q(r) \quad (\text{B.11})$$

$$p_{24} = Q(3r) \quad (\text{B.12})$$

Hence the average bit error probability is

$$P_b(E) = \frac{1}{4} \left(3 Q(r) + 2 Q(3r) - Q(5r) \right). \quad (\text{B.13})$$

It follows from (B.13) that for a bit error rate of 10^{-5} , a four-level MSK requires 13.4 dB E_b/N_0 . Thus in achieving twice bandwidth efficiency of biorthogonal MSK, the four-level MSK requires about 142% increase in the average bit energy; whereas with Q^2PSK the increment is only 45%. Thus Q^2PSK turns out to be a more energy efficient candidate to increase the bandwidth efficiency by a factor of two over ordinary or biorthogonal MSK.

APPENDIX C

SUFFICIENT STATISTIC FOR DECISION IN

CODED Q²PSK

In chapter four, demodulation of coded Q²PSK signal was based on hard decision as shown in Figure 4.1. The meaning and definitions of different symbols and variables used in the following discussions are consistent with Figure 4.1. As shown in this figure, the decision about the information bits in $a_1(t)$ and $a_3(t)$ are made independently from the observations on the respective pulse trains only. To make a decision about a_2 , we make a simplifying assumption that a_1 and a_3 are decoded correctly. Correctly made decisions of a_1 and a_3 alongwith the estimates a_{2r} of a_2 and its redundant version a_{4r} of a_4 are then the observations for making decision about a_2 . A decoder, which is optimum in the sense of minimizing the probability of error, will maximize aposteriori probability given by

$$p(a_2 = a_1 a_3 a_{2r} a_{4r}) \quad (C.1)$$

In other words, the decoder choses $a_2 = +1$ if

$$p(a_2 = 1 | a_1, a_3, a_{2r}, a_{4r}) - p(a_2 = -1 | a_1, a_3, a_{2r}, a_{4r}) > 0 \quad (C.2)$$

and $a_2 = -1$ otherwise.

Let us write

$$a_{ir} = a_i + n_i \quad i = 1, 2, 3, 4$$

where a_i and n_i are the signal and noise components in the received sample a_{ir} .

Now (C.2) can be rewritten as

$$p(a_2=1 | a_{2r}, \{a_{4r} = -\frac{a_1}{a_3} a_2 + n_4 | a_1, a_3\}) - p(a_2=-1 | a_{2r}, \{a_{4r} = -\frac{a_1}{a_3} a_2 + n_4 | a_1, a_3\}) \geq 0$$

If probability of $a_2 = +1$ and $a_2 = -1$ are same and equal to half then the decoding rule reduces to

$$p_{n_2}(a_{2r} - 1) p_{N_4}(A_{4r} - 1) - p_{n_2}(a_{2r} + 1) p_{N_4}(A_{4r} + 1) \geq 0 \quad (C.3)$$

where,

$$A_{4r} = -\frac{a_1}{a_3} a_{4r}$$

$$N_4 = -\frac{a_1}{a_3} n_4$$

and p_{n_2} and p_{N_4} are the probability density functions of the random variables n_2 and N_4 , and the arguments of $p_{n_2}(\cdot)$, $p_{N_4}(\cdot)$ are the values of the random variables $(a_{2r}, \pm 1)$, $(A_{4r}, \pm 1)$ respectively (retaining the same notations for the random variables and the corresponding random values). Each of these two density functions are normal with variance $N_0/2$. After simplifying (C.3), one can write the optimum decoding rule as follows:

Choose $a_2 = 1$ if

$$V = a_{2r} - \frac{a_1}{a_3} a_{4r} \geq 0 \quad (C.4)$$

and $a_2 = -1$ otherwise.

Thus the optimum decoding is based on the observation V . Hence V is the sufficient statistic

REFERENCES

REFERENCES

- (1) Claude E. Shannon, "Communication in the presence of noise," *Proc. IRE* 37, No.1, pp.10-21, January 1949.
- (2) H. Nyquist, "Certain topics on telegraph transmission theory," *Trans. AIEE*, Vol. 47, pp. 617-644, April 1928.
- (3) Subbarayan Pasupathy, "Minimum shift keying: a spectrally efficient modulation," *IEEE Communications Magazine*, pp. 14-22, July 1979.
- (4) F. de Jager and C. B. Dekker, "Tamed frequency modulation, A novel method to achieve spectrum economy in digital transmission," *IEEE Trans. Commun.*, Vol. COM-26, pp. 534-542, May 1978.
- (5) Mark C. Austin and Ming U. Chang, "Quadrature Overlapped Raised-Cosine Modulation," *IEEE Trans. Commun.*, pp.237-249, Vol.Com-29, No.3, March 1981.
- (6) A. Lender, "The Duobinary technique for high speed data transmission," *IEEE Trans. Commun. Electron*, Vol. 82, pp. 214-218, May 1963.
- (7) J.G. Smith, "Spectrally efficient modulation," *Proc. IEEE Int. Conf. Commun.*, June 1977, pp.3.1.37 - 3.1.41.
- (8) M.K.Simon, "A generalization of minimum-shift-keying (MSK) type signaling based upon input data symbol pulse shaping," *IEEE Trans. Commun.*, Vol.Com-24, pp.845-856, Aug.1976.

- (9) S. A. Gronemeyer and A. L. McBride, " MSK and offset QPSK modulation,"
IEEE Transaction on Communications, Vol. Com-24, pp.809-820, Aug.1976.
- (10) Dirk Mulwijk, "Correlative phase shift keying - a class of constant envelope
modulation techniques," IEEE Transactions on Communications, Vol.
COM-29, No. 3, March 1981.
- (11) S. Pasupathy, "Correlative coding; A bandwidth efficient signaling scheme,"
IEEE Commun. Soc. Mag., Vol. 17, pp. 4-11, July 1977.
- (12) Adam Lender, "Method and apparatus for converting binary information
into a single-sideband 3-level correlative signal," US patent no. 4,406,009.
Sep. 20, 1983.
- (13) H.J. Landau and H.O.Pollak, " Prolate spheroidal wave functions, Fourier
analysis and uncertainty-III: The dimensions of the space of essentially time
and band limited signals, " BSTJ.,41,pp.1295-1336,July 1962.
- (14) D. Saha, " Q^2 PSK - A new spectrally efficient modulation scheme , " Proc.
Twenty first Annual Allerton conference on Communication ,Control, and
Computing, Univ. of Illinois, October 1983.
- (15) Debabrata Saha and Theodore G. Birdsall, "Quadrature-Quadrature phase
shift keying: a constant envelope modulation scheme " Proc. Conf. on Infor-
mation Sciences and Systems, Princeton, March 1986.
- (16) Debabrata Saha, " Quadrature-quadrature phase shift keying, " US patent
(to be issued).

- (17) J.M. Wozencraft and I.M. Jacobs, Principle of Communication Engineering , John Wiley and Sons,1965.
- (18) W.B. Davenport Jr. and W.L. Root, An introduction to the theory of random signals and noise, Mc.Graw - Hill Book Co., New York,1968.
- (19) W.C. Lindsey and M.K. Simon, Telecommunication Systems Engineering, Prentice-Hall, Englewood Cliffs, N.J.,1973.
- (20) D.P.Taylor, S.T. Ogletree, H.C. Chan and S.S. Haykin, " A high speed digital modem for experimental work on the communication technology satellite," Can. Elec. Eng. J., Vol. 2, no. 1, pp. 21-30,1977.
- (21) R.DeBuda, "Fast FSK signals and their demodulation," Can. Elec. Eng. J., Vol. 1, no. 1, pp. 28 - 34, 1976.
- (22) Rudi deBuda and Charles E. Jagger, "Self-synchronization circuit for a FFSK or MSK demodulator," US Patent no. 4,384,357, May 17, 1983.
- (23) Carl-Erik Sundberg, "Continuous phase modulation: A class of jointly power and bandwidth efficient digital modulation schemes with constant amplitude," IEEE Communications Magazine, Vol. 24, No. 4, pp.25-38, April 1986.
- (24) Golomb S.W., Digital Communications with Space Application, Prentice-Hall, Englewood Cliffs, N.J., 1964.
- (25) D. Saha and S.Pasupathy, " Fractional sampling rate demodulation of FSK signals," Journal of the Franklin Institute, Vol. 311, No. 1, 1981, March, 1984.

- [26] Jerrold A. Heller and Irwin Mark Jacobs, "Viterbi decoding for satellite and space communication," *IEEE Transactions on Communication Technology*, Vol. COM-19, no.5, October 1971.
- [27] Gottfried Ungerboeck, "Channel coding with multilevel phase signals," *IEEE Transactions on Information Theory*, Vol. IT-28, No. 1, January 1982.

END

FEB.

1988

DTIC